



Lithium Ion Capacitors in Organic Electrolyte System: Scientific Problems, Material Development, and Key Technologies

Pengxian Han, Gaojie Xu, Xiaoqi Han, Jingwen Zhao, Xinhong Zhou, and Guanglei Cui*

Lithium ion capacitors (LICs), which are hybrid electrochemical energy storage devices combining the intercalation/deintercalation mechanism of a lithium-ion battery (LIB) electrode with the adsorption/desorption mechanism of an electric double-layer capacitor (EDLC) electrode, have been extensively investigated during the past few years by virtue of their high energy density, rapid power output, and excellent cycleability. In this review, the LICs are defined as the devices with an electrochemical intercalation electrode and a capacitive electrode in organic electrolytes. Both electrodes can serve as anode or cathode. Throughout the history of LICs, tremendous efforts have been devoted to design suitable electrode materials or develop novel type LIC systems. However, one of the key challenges encountered by LICs is how to balance the sluggish kinetics of intercalation electrodes with high specific capacity against the high power characteristics of capacitive electrode with low specific capacitance. Herein, the developments and the latest advances of LIC in material design strategies and key techniques according to the basic scientific problems are summarized. Perspectives for further development of LICs toward practical applications are also proposed.

1. Introduction

Human development is inseparable from the supply of energy. The history of human civilization is a history of energy utilization. People have never stopped exploring energy from natural resources. Coal, oil, etc., have already promoted the first and the second industrial revolution. However, with the rapid development of economy, the way to obtain energy at the

expense of environment has long been criticized. Atomic energy and computer technology have been well developed during the third industrial revolution. The fourth industrial revolution which is represented by mobile electronics, electric vehicles, energy interconnection, etc., have brought people into a new era powered by wind energy, water energy, solar energy or other renewable energy sources. Correspondingly, the development of environmentally friendly electrochemical energy storage devices is becoming global concerns.^[1,2]

In the past few years, the electrochemical energy storage devices represented by lithium-ion batteries (LIBs) and electric double-layer capacitors (EDLCs) have been made great progress.^[3–8] The advanced LIBs can store energy densities of 150–200 Wh kg⁻¹ in nonaqueous liquid electrolyte and >300 Wh kg⁻¹ in solid state electrolyte.^[9,10] However, the power output

(<1 kW kg⁻¹) and lifespan (<10⁻³ times) are somewhat unsatisfactory, especially for the novel solid state LIBs. On the contrary, the power density and the lifespan of EDLCs can reach to >5000 W kg⁻¹ and >100 000 times, respectively, but the energy density is <10 Wh kg⁻¹ in organic electrolyte and much lower in aqueous electrolyte.^[11,12] The noticeable difference between LIBs and EDLCs in relation to their energy density, power density and calendar life can be ascribed to their different energy storage mechanisms. In LIBs, the energy is electrochemically stored/released by means of the intercalation/deintercalation of lithium ions into the crystal lattice of the electrode materials both at anode and cathode (Figure 1a), whereas in EDLCs, the charges are physically stored/released by the adsorption/desorption of ions on porous carbon with high specific surface area (typically activated carbon, AC) (Figure 1b). Different electrochemical kinetics lead to different energy storage performances. Electrochemical kinetics of the ion intercalation into the electrodes is much slower than physically adsorption of ions on the surface of the electrodes.

With the ever-increasing development of energy recovery systems or start power in transportation systems, high performance energy storage devices with high energy density, high power density, excellent cycleability and high safety are urgently needed. Under such circumstances, an advanced energy storage device, lithium-ion capacitors (LICs), a hybrid electrochemical

P. Han, G. Xu, X. Han, Dr. J. Zhao, Prof. G. Cui
Qingdao Industrial Energy Storage Research Institute
Qingdao Institute of Bioenergy and Bioprocess Technology
Chinese Academy of Sciences
Qingdao 266101, P. R. China
E-mail: cuigl@qibebt.ac.cn

X. Han
University of Chinese Academy of Sciences
Beijing 100049, P. R. China

Prof. X. Zhou
College of Chemistry and Molecular Engineering
Qingdao University of Science and Technology
Qingdao 266042, P. R. China

The ORCID identification number(s) for the author(s) of this article can be found under <https://doi.org/10.1002/aenm.201801243>.

DOI: 10.1002/aenm.201801243

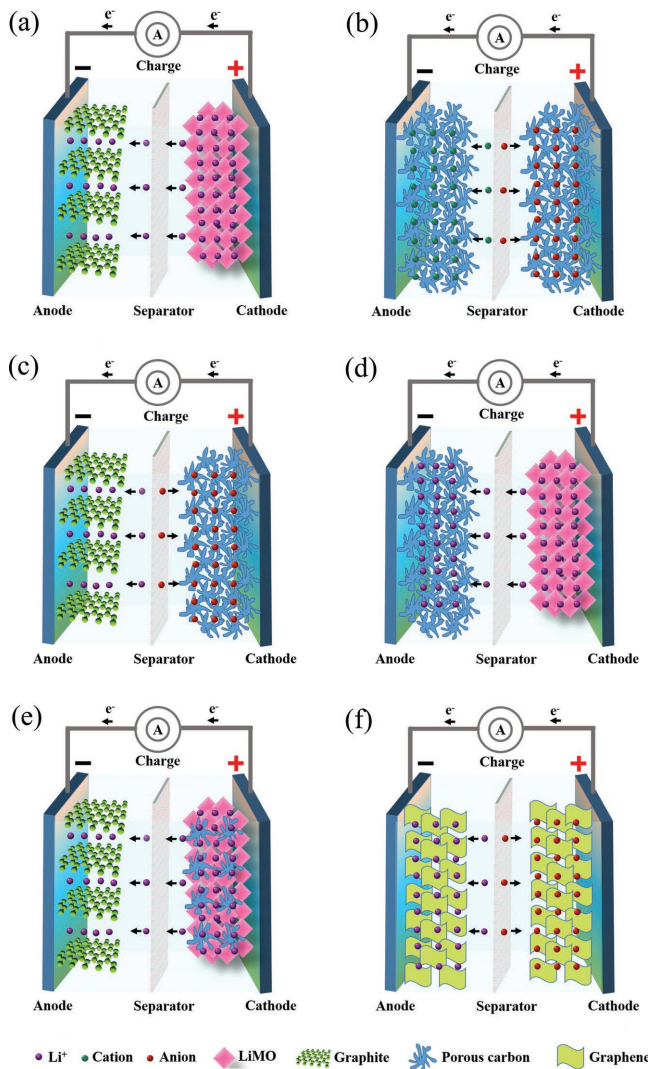
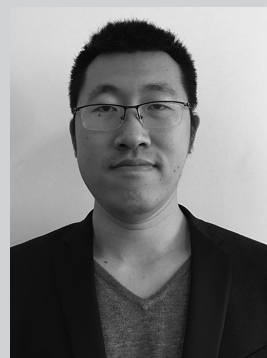


Figure 1. Cell structure and charge storage mechanisms of the three electrochemical energy storage devices: a) LIBs, b) EDLCs, and c–f) LICs with different work mechanisms, which are 1) electrochemical intercalation (−)//physical adsorption (+), 2) physical adsorption (−)//electrochemical intercalation (+), 3) electrochemical intercalation (−)//physical adsorption + electrochemical intercalation (+), and 4) symmetrical LICs and graphene based LICs, respectively.

energy storage device combining the lithium ion intercalated electrode of LIBs with the ion adsorption electrode of EDLCs is proposed and developed.^[13–16] When the LICs are charged, the energy are stored in the electrodes by ion adsorption on the capacitive cathode and lithium ion intercalation into the anode, respectively (Figure 1c). Consequently, the operating voltage window of the LICs is enlarged by performing the two electrode in different potential ranges, which result in improved energy density, acceptable power density, satisfactory cycle performance and wide operating temperature range.^[17,18] Throughout the research history of LICs, the LICs can be generally classified as the following types based on different active materials and mechanisms in this review (as shown in Figure 1c–f): 1) electrochemical intercalation (−)//physical adsorption (+), for example, titanium-based compound (−)//porous carbon (+),^[19–22]



Pengxian Han is currently an associate professor at Qingdao Institute of Bioenergy and Bioprocess Technology, Chinese Academy of Sciences, China. He received his M.S. degree in chemistry from Tianjin University in 2007. He then worked as a Senior R & D Engineer at BYD Company Limited (Shenzhen, China). His research interests include advanced materials for energy storage and conversion devices.



Gaojie Xu is currently a research associate at Qingdao Institute of Bioenergy and Bioprocess Technology, Chinese Academy of Sciences, China. He received his M.S. degree in applied chemistry from Ocean University of China in 2012. His research interests mainly concentrate on advanced electrolytes (additives) and separators for Li-ion batteries and Li-ion capacitors.



Guanglei Cui obtained his Ph.D. degree at the Institute of Chemistry, Chinese Academy of Sciences, in 2005. From 2005 to 2009, he had worked at Max-Planck-Institute for Polymer Research and Max-Planck-Institute for Solid State research as a post-doctoral scientist on Energy Chemistry Project. Currently he is a principal investigator at Qingdao Institute of Bioenergy and Bioprocess Technology, Chinese Academy of Sciences. His research topics include sustainable and highly efficient energy-storage materials, and novel energy devices.

graphite(−)//porous carbon (+),^[23] silicon-based composites (−)//porous carbon (+)^[24–26] and metal oxide (−)//porous carbon (+),^[27–29] etc.; 2) physical adsorption (−)//electrochemical intercalation (+), for example, AC (−)//LIB cathode material,^[30] etc.; 3) electrochemical intercalation (−)//physical adsorption + electrochemical intercalation (+), for example, graphite or hard carbon (−)//LIB cathode material-AC (+),^[31] Li₄Ti₅O₁₂ (−)//LIB cathode material-AC (+),^[32] etc.; 4) symmetrical LICs and graphene based LICs,^[33–36] i.e., both of the electrochemical intercalation and physical adsorption mechanisms are acted on cathode and anode simultaneously.

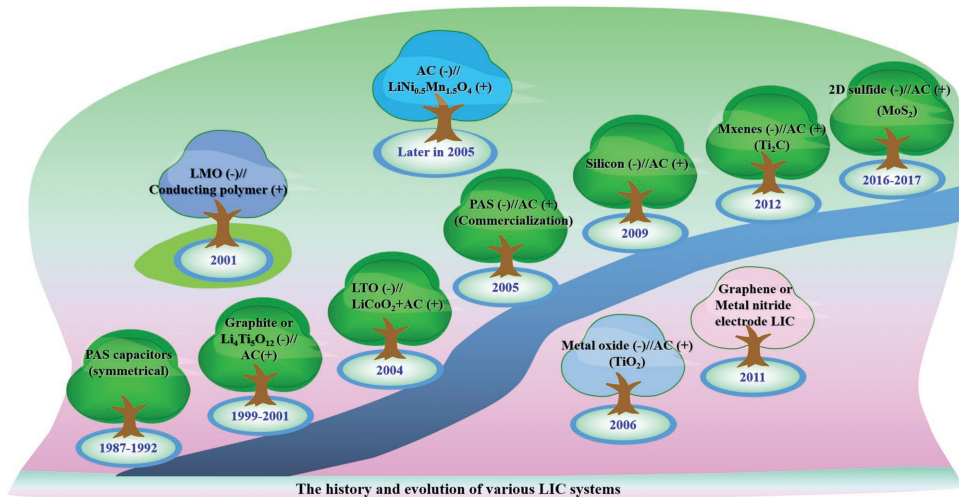


Figure 2. The history and evolution of various LIC systems.

In retrospect of LICs, it cannot but start from the study of polyacenic semiconductor (PAS). **Figure 2** presents the history and evolution of various LIC systems. In 1987, Yata et al. first found the intercalation behavior of lithium ion into PAS in $1\text{ M LiClO}_4/\text{sulfolane}+\gamma\text{butyrolactone}$ electrolyte.^[37] Then, in 1989, coin-type PAS capacitors (2.5 V) with a capacity two or three times higher than EDLCs, which employed the PAS as the active materials both the cathode and anode electrodes, were commercialized by Shizukuni Yata (Kanebo Ltd., Japan).^[38] Up to 1992, the working voltage of PAS capacitors was increased to 3.3 V by the first application of prelithiation strategy toward PAS anode.^[39] Based on the above studies, a hybrid capacitor by coupling an AC cathode with a graphite anode in a lithium ion organic electrolyte was proposed in 1999 by Morimoto, T.^[40,41] The maximum applicable voltage of this hybrid capacitor was over 4.2 V. Almost at the same time, another type of hybrid capacitor consisting of a nanosized $\text{Li}_4\text{Ti}_5\text{O}_{12}$ (LTO) anode with an AC cathode was first proposed by Amatucci's group, which was a 2.8 V cell with energy density of $>10\text{ Wh kg}^{-1}$.^[42] Simultaneously, they also first investigated the electrochemical performance of lithium metal oxide (LMO) (-)//conducting polymer (+) LICs. In 2004, Amatucci et al. introduced an LTO (-)// $\text{LiCoO}_2\text{-AC}$ (+) system and opened the door of using LIB cathode materials in LIC system.^[43] Afterward, Prof. Naoyuki Kondo took great efforts to develop LTO based Li-ion hybrid capacitors.^[44,45] The “lithium-ion capacitor” was eventually named by Ando et al. based on the prelithiation method.^[46] The negative

active material of this LICs was a prelithiated PAS material. In 2005, Fuji Heavy Industry commercialized the LICs based on prelithiated PAS anode and porous carbon cathode using laminated structure. Then, other companies, including Advanced Capacitor Technologies, JM Energy Corporation, FDK Lithium Ion Capacitor Co., Ltd, TAIYO YUDEN Co., Ltd, General Capacitor Intl, Inc., Ling Rong New Energy Technology (Shanghai) Co., Ltd. also made great efforts toward the commercialization of LICs based on different technology roadmaps.^[47] **Table 1** lists the product features of some state-of-the-art commercially available LICs. The energy density of these LIC devices range from 10 to 18 Wh kg^{-1} . The cycle number can reach to above tens of thousands of times. In 2005, AC materials were used as anode in $\text{AC}(-)/\text{LiNi}_{0.5}\text{Mn}_{1.5}\text{O}_4(+)$ LIC system.^[48] Then in 2006, Brousse' group and Li group first proposed a novel $\text{TiO}_2(-)/\text{AC}(+)$ LIC system utilizing metal oxide.^[49,50] With the march on fundamental research and technical respects, more and more types of LICs were developed. As an excellent anode material, silicon based material was first used in LIC in 2009.^[51] In 2011, a graphene surface-enabled lithium ion-exchanging capacitor was proposed, which opened the door for the application of graphene materials in LICs.^[52] In the meantime, Cui's group unprecedently developed a series of metal nitride based LICs.^[53-57] Until 2012, another typical 2D Mxene, Ti_3C , was first used as negative electrode in a nonaqueous asymmetric cell in $1\text{ M LiPF}_6/\text{EC-DMC}$.^[58] Recently, the 2D materials have drawn wide attention. 2D sulfide based anode materials in LICs have

Table 1. The product features of some state-of-the-art commercially available LICs.

Company	Cell type	Work voltage [V]	Capacitance [F]	Energy density [Wh kg^{-1}]	Power density [kW kg^{-1}]	Cycle
JM Energy Corporation	Laminate	2.2–3.8	2100	10	–	800000
	Prismatic	2.2–3.8	3300	13	–	300000
TAIYO YUDEN	Cylinder	2.2–3.8	200	15	–	100000
General Capacitor Intl, Inc.	Laminate	2.2–3.8	3000	18	7.5	100000
Ling Rong New Energy Technology (Shanghai) Co., Ltd.	Laminate	4	15000	–	–	50000

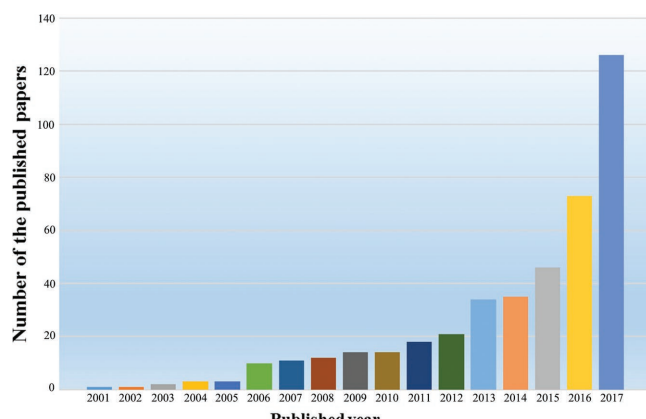


Figure 3. Nonaqueous LIC-related papers year by year in Web of Science Core Collection, date: 2017 December 31, search strategy: TOPIC: “lithium ion capacitor*” OR “lithium-ion capacitor*” OR “li-ion capacitor*” OR “hybrid capacitor*” OR “hybrid supercapacitor*” OR “hybrid battery capacitor*” OR “asymmetric supercapacitor *.” Timespan: 2001–2017.

been well studied since 2016.^[59,60] **Figure 3** shows the papers in relation to nonaqueous LICs in Web of Science Core Collection from 2001 to 2017. By 2012, the published papers increased steadily year by year. After 2015, the published papers were fiercely increased, reaching nearly 130 articles in 2017 (up to December), indicating that great progress has been made in the research of LICs during the past few years.

By analyzing all of the aforementioned types of LICs, there exist three main fundamental scientific problems, including:

- 1) Low kinetics of the electrochemical intercalation electrodes do not match the fast kinetics of the capacitive electrodes, which leading to a mismatched region of kinetics. Specifically, when the power density is low, the energy density is high. However, when the power density is high, the energy density is sharply decreased.
- 2) The high specific capacities of the electrochemical intercalation/deintercalation type electrodes do not match the low specific capacitances of the physical adsorption/desorption type electrodes, which lead to a hard job when balancing the different electrode materials.
- 3) The prelithiation strategy, which is a key technology to compensate for poor efficiency in the first charge/discharge cycle, receive a high operating voltage, reduce the electrode resistance, and decrease the electrolyte consumption during long term cycling.

In view of these key scientific problems, a large number of systematic, in-depth, and scientific research works on novel materials and prelithiation had been carried out. A series of strategies were proposed to improve the energy density, power density and cycleability, including:

- 1) Preparing anode materials with fast lithium ion intercalation/deintercalation. The strategies contain: i) nanostructuring and morphological control;^[61] ii) surface coating with high electrical conductive materials;^[62] iii) elemental doping with heterogeneous elements;^[63,64] or iv) formation of composite,^[65–67] etc.

- 2) Designing cathode materials with high specific capacity/capacitance. The strategies contain: i) high specific area with proper porous structure;^[68–70] ii) elemental doping, such as nitrogen doping;^[71] iii) multidimensional design porous structure;^[72–75] iv) biomass- or polymer-derived porous carbon.^[76–79]
- 3) Developing high effective prelithiation technologies. The strategies contain: i) short-circuiting metallic lithium with anodes externally;^[80,81] ii) short-circuiting using a suitable resistor;^[82] iii) charging under proper current density;^[83] iv) using electrochemical irreversible lithium metal oxides as lithium resources to substitute the metallic lithium,^[84] or adding extra organic lithium salts into AC cathode and irreversibly providing Li⁺ to the anode during initial charging.^[85]

Outstanding achievements have been achieved toward LICs during the past few years, in relation to novel active materials, the design of electrodes, the innovation of novel LIC systems and the improvement of prelithiation strategies. In this review, the development of nonaqueous LICs and the latest advances of different material design strategies in various LIC systems are reviewed thoroughly and systematically. Future perspectives for further development toward practical applications are also proposed.

2. Titanium-Based Compound (−)//Porous Carbon LICs

2.1. LTO (−)//AC (+)

LTO has aroused much concern as a competitive anode material of LIBs in high power output fields due to its excellent characteristics, including: 1) a stable charge/discharge potential (≈ 1.55 V vs Li⁺/Li), 2) free of the formation of solid electrolyte interface (SEI) and lithium dendrite, 3) negligible volume variation during lithium ion intercalation/deintercalation, and 4) high coulombic efficiency (up to $\approx 100\%$).^[86,87] In 2001, Amatucci and co-workers first proposed the concept of nonaqueous asymmetric supercapacitors by coupling an AC cathode with a nanostructured LTO anode in a nonaqueous electrolyte.^[88] As shown in **Figure 4**, when it was charged, a PF₆⁻ double layer formed on the surface of the cathode (3–4.5 V vs Li⁺/Li) and the

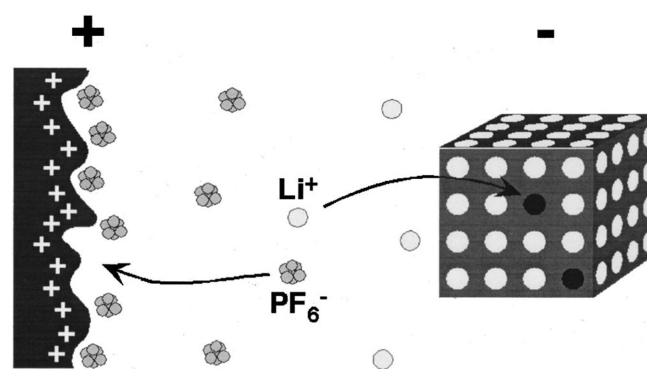


Figure 4. Simplified schematic of electrode reactions of an LTO (−)//AC (+) LIC. Reproduced with permission.^[88] Copyright 2001, The Electrochemical Society.

lithium ion intercalation into LTO crystalline (≈ 1.5 V vs Li^+/Li), thus enabling the cell to work at 1.5–3 V. Afterward, a 500 F plastic matrix bonded prototype device was also presented.^[89] The device had an usable packaged specific energy density of 11 Wh kg⁻¹ at 0.8 kW kg⁻¹. The cycle life is between 10000 and 100000 cycles on the basis of operation conditions.

Unfortunately, large-scale application prospects of LTO in LICs is hindered by some intrinsic kinetics problems, such as poor electrical conductivity ($\approx 10^{-13}$ S cm⁻¹) and sluggish Li^+ diffusion ($\approx 10^{-16}$ cm² s⁻¹), which greatly constrain the rate capability of these LICs. Much effort has been made to enhance the electrical conductivity. The strategies, including nanosizing, surface modification, elemental doping and compositing, are introduced in details as following.

2.1.1. Nanosizing LTO

An obvious advantage of the reduction in LTO particle size to the nanoscale is to improve the Li^+ diffusion kinetics. Nano-sized particles can drastically shorten the transport distance for both e^- and Li^+ , and significantly increases the electrode/electrolyte soakage area, enabling high charge/discharge rate and long cycle life. In view of this, nanosized materials with different morphologies had been designed and synthesized.

In 2006, Xia et al. prepared a kind of nanosized LTO by molten salt method. The particle-size distribution was ≈ 100 nm and could be adjusted by optimizing the synthetic condition. The nanosized LTO//AC LIC showed much better rate capability within the voltage of 1.5–2.8 V. Moreover, the discharge capacity retention of 100 C/3 C was as high as 60%.^[90] On the basis of similar strategy, Sun et al. also prepared a ≈ 900 nm spherical LTO with a higher tap density. This LTO//AC LIC could deliver 41.7 Wh kg⁻¹ at 468.7 W kg⁻¹ at 1.0–3.5 V.^[91] Recently, Lee et al. prepared a ≈ 5 mm granule

LTO with primary particles ranging from 300 to 500 nm. It had abundant porous structure, which was beneficial for liquid electrolyte soakage. Even after 10000 cycles, the Coulombic efficiency was still remained at 97.4%.^[92]

2.1.2. Surface Coating of LTO

Although nanostructuring is an effective way to improve the LTO electrode kinetics, there are still some other disadvantages at the same time. First, the tedious synthesis process and the mixing of the electrode slurry are very sensitive to experimental conditions. Second, the reduction in particle size will increase the specific surface area of the electrode, and then in turn increase the risk of side reaction between the electrolyte and the electrode, resulting in an unsatisfactory cycle performance. Third, the volumetric energy density of the device will be decreased due to the decrease of material tap density.^[93] Surface coating is an reliable method to enhance the surface electronic conductivity by forming a thin layer of conductive materials, meanwhile, the electrolyte decomposition LTO electrode can also suppressed (Figure 5).^[94] Conventionally, carbon coating is the best choice considering cost-effectiveness aspects.

In 2007, Xia et al. proposed a thermal vapor decomposition strategy to cover an uniform graphitic carbon on LTO particles.^[95] Then a carbon layer with 5 nm thick was formed, the electrical conductivity was increased to 2.05 S cm⁻¹ and the charge-transfer resistance for lithium-ion intercalation was reduced. As a negative electrode for the LTO//AC LIC, it kept 50% of initial capacity in comparison with that of 29% of the raw LTO at the rate of 24 C. Gao et al. designed a carbon modified LTO by in situ carbon coating.^[96] The carbonization of organic precursors formed an intimate in situ carbon film on LTO particles to improve the mobility of electrons. The LTO-C//

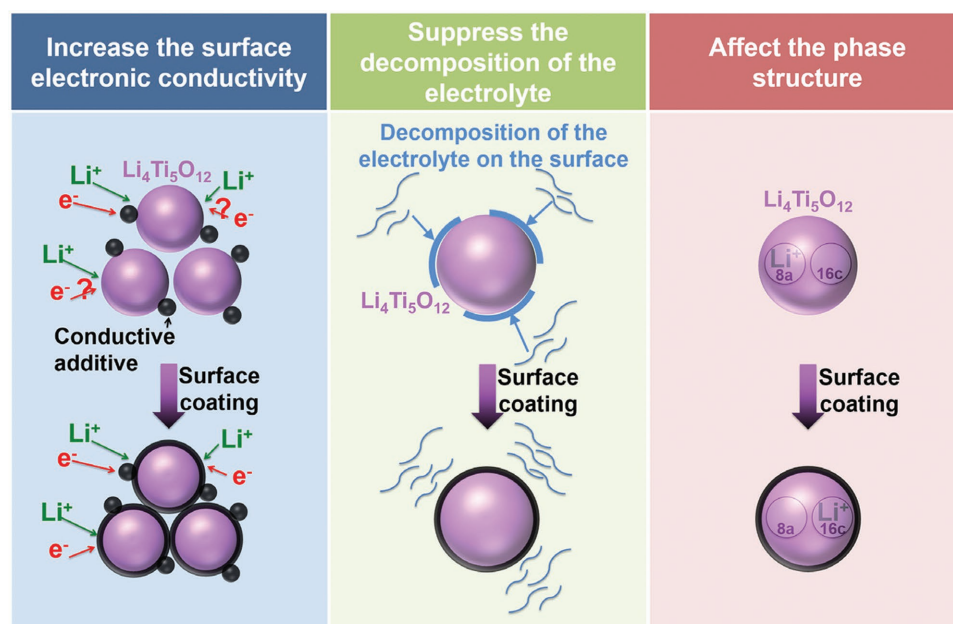


Figure 5. Schematic illustration of the merits of surface coating on LTO-based materials. Reproduced with permission.^[94] Copyright 2015, Elsevier.

AC LIC could be well operated at 30 C rate and 80% capacity was kept even after 9000 deep cycles.

Carbon coating can also improve the tap density of LTO. Scrosati et al. developed a kind of LTO microsphere particles coated by a thin film of pitch-based carbon using hydrothermal method.^[93] The tap density of the obtained C-LTO particles was 150% higher than that of the carbon-free LTO. The C-LTO electrode could deliver 142 mAh g⁻¹ even at 50 C. The energy density of the LTO-C//AC LIC was as high as 57 Wh L⁻¹ at 100 W L⁻¹. The high volumetric energy density was ascribed to the high tap density of C-LTO material. Rajagopal et al. used camphor as a carbon source and synthesized carbon grafting LTO material.^[97] The best electrochemical performance was obtained for the sample of 10 wt% carbon content (LC-10). LC-10 electrode could deliver an energy density of 330 mWh L⁻¹ at 2.8 kW L⁻¹. There was no capacity decay even after 4000 cycles by virtue of the presence of porous carbon layer improving the elastic properties of the electrode and preventing crack formation during the cycling. Recently, Huang' group developed an LIC using LTO/C composite as anode and 3D porous graphene macroform (PGM) as cathode (Figure 6).^[98] A ≈4 nm thick carbon layer was coated on LTO. The PGM was prepared using hydrothermal and freeze drying of graphene oxide. After optimizing working voltage and the electrode material formula, the LIC could offer an energy density of 40 Wh kg⁻¹ at 8.3 kW kg⁻¹.

2.1.3. Element Doping of LTO

In comparison with carbon coating, element doping could adjust the electronic structure of LTO, resulting in improved electrical conductivity and a superior Li⁺ intercalation/deintercalation behavior. Yoon et al. synthesized Al³⁺, Cr³⁺, or Mg²⁺-doped LTO powders by using conventional solid-state reaction.^[99] It was very interesting that Cr³⁺ and Mg²⁺ dopants enhanced the conductivity of LTO due to the formation of mixed Ti⁴⁺/Ti³⁺ valences, whereas Al³⁺ substitution improved the discharge capacity and cycleability of LTO because of the stronger

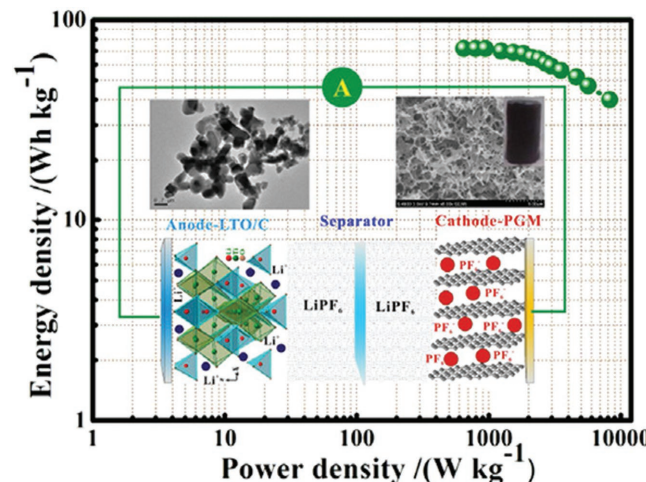


Figure 6. Ragone plots of PGM (+)//carbon-coated LTO (-) LIC. Reproduced with permission.^[98] Copyright 2015, Elsevier.

valence bond of Al–O in comparison with Ti–O. Zhang et al. developed a trivalent Ti self-doped LTO, which could enhance the electrical conductivity by reducing the Li⁺ diffusion length and facilitating electron transfer, leading to an improved rate capability (Figure 7).^[100] Then an LIC was fabricated by coupling this Ti self-doped nanostructured LTO anode with peanut shell based AC cathode, delivering an energy density of 67 Wh kg⁻¹ at 8 kW kg⁻¹ between 1–3 V. After 5000 cycles at 0.5 A g⁻¹, the capacity retention was as high as 79%.

2.1.4. Preparation of LTO Composite

The electrochemical properties of LTO can also be enhanced by preparing a series of LTO-based composites using a second component. The second components should be high conductivity and chemical stability. Thus, both of electronic conductivity and Li⁺ conductivity could be promoted. Thus, the extra conductive additives in the slurries of the electrode could be decreased or even discarded completely.

2.1.5. Composite LTO@1D Carbon Nanofiber or Nanotube

Carbon nanofiber (CNF) and carbon nanotube (CNT) are two kinds of excellent 1D carbonaceous conductive agents. The unique structures and physical properties endow them with good electronic conductivity, extended electrochemical window and excellent chemical stability. They have been extensively used as electron conducting channels in the modification of electrode materials. Naoi et al. developed a novel nanocrystalline LTO-grafted carbon nanofibers (nc-LTO/CNF) by way of ultracentrifuging (UC) method (Figure 8).^[45,47] The electronic conductivity of nc-LTO/CNF was up to 25 S cm⁻¹. Consequently, the nc-LTO/CNF anode with a AC cathode significantly enhanced both of the power and energy density. The LIC could deliver an energy density of 40 Wh L⁻¹ and power density of 8 kW L⁻¹ when the weight ratio of LTO/CNF was 70/30. Afterward, they also developed a hyper-networked LTO/carbon hybrid nanofiber sheets.^[101] The nanofiber sheets were prepared by electrospinning coupled with vapor polymerization. By forming a 3D conductive network, the electrical conductivity of the composite were highly strengthened. The LIC exhibited a high energy density of 22 W kg⁻¹ at 4 kW kg⁻¹.

On the basis of the similar conception, Park et al. developed LTO-AC hybrid nanotubes as anodes using electrospinning techniques, an in situ TiO₂ sol-gel reaction followed by hydrothermal reaction and heat treatment.^[102] The large specific surface area of the AC enabled this complementary electrode system to be operated with high electrical conductivity and short ion diffusion length. In especial, 1D-tubular structure facilitated the electrolyte to access the active material surface and was favorable for Li⁺ transport kinetics. Such a hybridized electrode could store and release charges by faradaic and nonfaradaic mechanisms simultaneously. When the such hybrid nanotube anodes were coupled with AC cathode, a satisfactory energy density of 32 Wh kg⁻¹ was delivered at 6 kW kg⁻¹. Then, Huang et al. developed a highly porous LTO/C nanofiber (PLTO-C) material through electrospinning and a post-two-step annealing treatment (Figure 9).^[103]

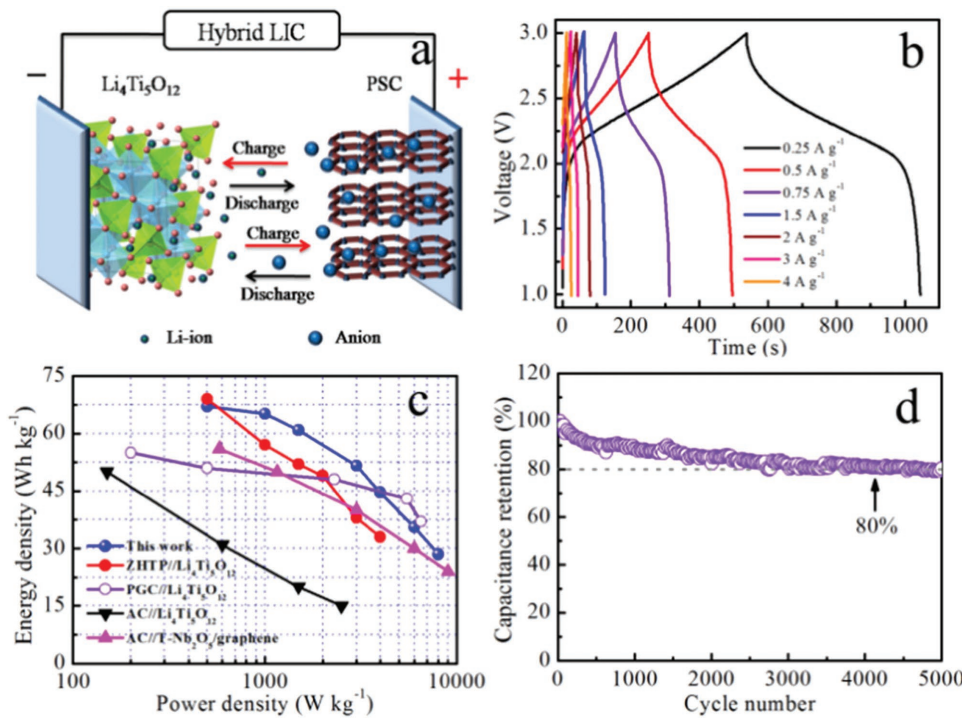


Figure 7. a) Schematic illustration of Ti self-doped LTO (−)// peanut shell based AC (+) LICs. b) Charge/discharge curves under different current densities. c) Ragone plots of Ti self-doped LTO (−)// peanut shell based AC (+) LIC and other hybrid LICs in previous reports. d) Cycle performance at 0.5 A g⁻¹ for 5000 cycles. Reproduced with permission.^[100] Copyright 2015, Elsevier.

The optimal carbon content could improve the electronic conductivity of LTO without sacrificing the overall energy storage capacity. Moreover, both nanosized pores and LTO nanocrystals in the LTO/C hybrid could facilitate the electrolyte infiltration, enabling full utilization of LTO and fast transport of Li⁺ and e⁻. The PLTO/C based LIC could deliver about 27.5 Wh kg⁻¹ at 3 kW kg⁻¹ with a voltage range of 0.5–2.5 V.

2.1.6. Composite of LTO@2D Graphene

Graphene, a new 2D carbonaceous material, has aroused wide attention due to its excellent electronic conductivity.^[104] By virtue of high specific surface area, outstanding mechanical properties, it is generally used as a good conductive additive to the composite electrode materials in electrochemical

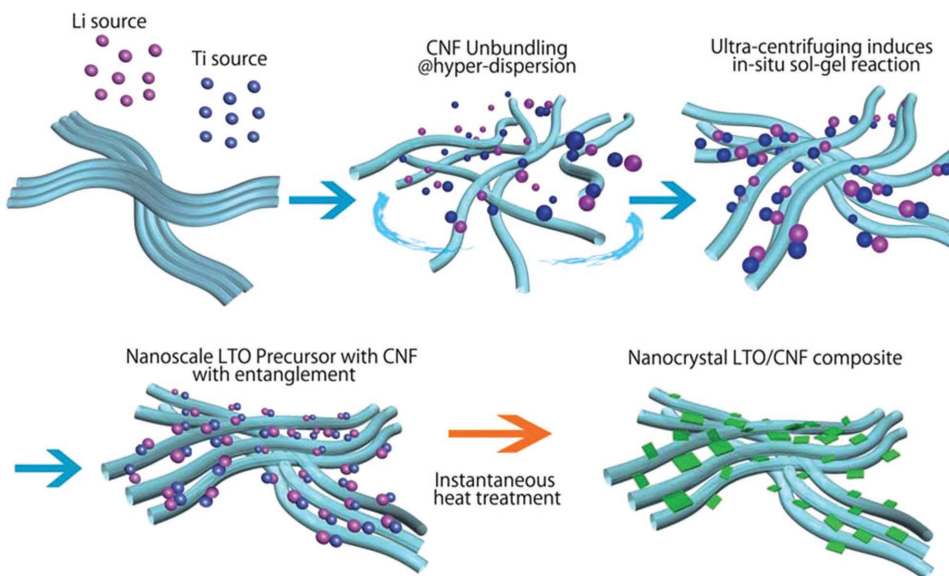


Figure 8. The design of a UC treatment. It involved a one-step rapid generation scheme, producing various nanocomposites being able to store and deliver energy at the maximized capacity with excellent rate capability. Reproduced with permission.^[47] Copyright 2012, Royal Society of Chemistry.

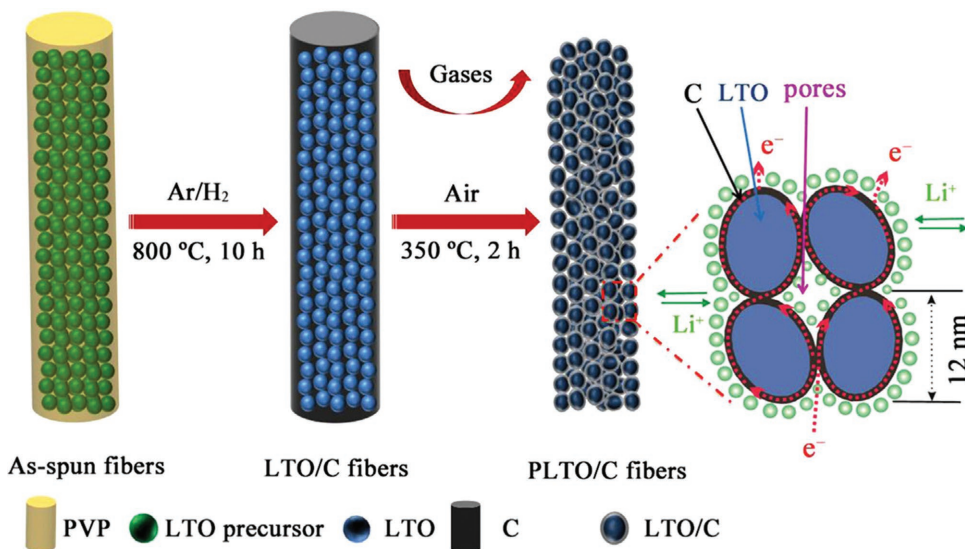


Figure 9. Diagram of the synthesis of the PLTO/C nanofibers through electrospinning and a post-two-step annealing treatment. Reproduced with permission.^[103] Copyright 2014, Elsevier.

energy storage devices.^[105] The formation of 2D continuous and highly conductive network of graphene can dramatically improve electronic conductivity and shorten the ion transport path of LTO. Second, it is also good for the rapid Li^+ diffusion because graphene can effectively limit the crystalline growth of the spinel LTO. Lastly, the dispersed LTO nanoparticles can suppress the agglomeration and restacking of graphene. Kang et al. described a novel LIC by coupling a graphene-wrapped LTO anode with an AC cathode.^[106] The anchoring of LTO on graphene could significantly promote the electronic conductivity of LTO. The LIC could deliver 15 Wh kg^{-1} and offer a power density of nearly 2.5 kW kg^{-1} . Ma et al. reported a 3D crumpled graphene sheets wrapped nano-LTO (LTO@GS) composites using inexpensive and environmentally titanium oxide as a starting material.^[107] When LTO@GS (1.93%) was served as an anode electrode, the LTO@GS//AC LIC delivered 13.4 Wh kg^{-1} at 1782.7 W kg^{-1} between $1.5\text{--}3\text{ V}$. 90% of its initial capacity could be held even after 20000 deep cycles at 80 C rate. Recently, various strategies were also applied to synthesize LTO-graphene nanocomposites as anode materials of LIC, including sol-gel method,^[108,109] one-step synthesis strategy,^[110] solid state reaction,^[111] and so on.

2.2. LTO (-)//Other Type of Porous Carbon (+)

Apart from the enhancement of LTO anode, the development of advanced porous carbon cathode is also of importance. One of great challenges is to promote the specific capacity of the porous carbonaceous cathode. Recently, various porous carbon materials had been explored by different method using different carbon sources.^[112-114] These materials exhibited higher specific capacity than that of commercial AC ($\approx 100\text{ F g}^{-1}$ or $< 50\text{ mAh g}^{-1}$ in lithium ion

based electrolytes). As a typical case, a porous graphitic carbon (PGC) derived from mesocarbon microbeads with “core-shell” structure was designed.^[115] The inner core was porous amorphous carbon and the outer shell was graphitic carbon. The porous structure offered sufficient reaction sites and was beneficial for ion diffusion. Meanwhile, the outer graphitic shells could facilitate the electron transportation. The IR-drop of PGC cathode was about 14 times lower than that of commercial AC cathode. The LTO//PGC LIC delivered an energy density of 37 Wh kg^{-1} even at 6.5 kW kg^{-1} , which was almost double that of the LTO//AC LIC.

2.2.1. LTO (-)//Graphene Based Porous Carbon (+)

In 2012, Ruoff et al. developed an activated microwave expanded graphite oxide (a-MEGO), which had small sizes of $< 10\text{ nm}$ and an specific surface area of $3100\text{ m}^2\text{ g}^{-1}$.^[116] The specific capacitance of a-MEGO in lithium-based electrolyte was up to 182 F g^{-1} ($\approx 125\text{ mAh g}^{-1}$) at 1.1 A g^{-1} . The LTO//a-MEGO type LIC could show an encouraging energy density of 40.8 Wh kg^{-1} . Aravindan et al. reported that the specific capacity of the trigol reduced graphene oxide (TRGO) nanosheets in similar lithium-based electrolyte was 58 mAh g^{-1} .^[117] The LTO//TRGO LIC device was able to deliver an energy density of 45 Wh kg^{-1} and a power density of 3.3 kW kg^{-1} and presented a satisfactory cycleability as high as 5000 cycles. Meng et al. prepared a nitrogen-doped graphene-based aerogel (NGA) composites by sol-gel polymerization combined with KOH activation process.^[118] Such a porous graphitic structure made the electrolyte ions much easier to permeate and diffuse and retained high electrical conductivity. Moreover, the nitrogen-doping could contribute pseudocapacitance and improve electrical conductivity. The LTO//NGA LIC provided an energy density of 21 Wh kg^{-1} even at 8 kW kg^{-1} .

2.2.2. LTO (-)//Biomass Derived Porous Carbon (+)

Most of the commercial high specific surface area AC contains a large fraction of micropores (<0.5 nm), which are not accessible to the larger ions. There exists an optimum balance between pore size and electrochemical performance.^[119] Biomass-derived porous carbonaceous materials have received enormous attentions in supercapacitors by virtue of tunable physical/chemical properties, environmental concern, and economic value.^[120–123] Aravindan et al. reported a coconut shell based AC with 60% mesoporous volume and high specific surface area of $1652\text{ m}^2\text{ g}^{-1}$ by hydrothermal activation process along with chemical activation.^[124] The maximum specific capacitance of 159 F g^{-1} was delivered in $1\text{ M LiPF}_6/(\text{EC+DMC})$. The LTO//coconut shell AC LIC could deliver an extremely high energy density of 69 Wh kg^{-1} between 1–3 V. They further prepared a *Prosopis juliflora*-derived AC. The AC was obtained by heat treatment at $900\text{ }^\circ\text{C}$ with a 1:2 KOH ratio (KC21-900). The specific surface area of KC21-900 AC was up to $2410\text{ m}^2\text{ g}^{-1}$. Moreover, its specific capacitance reached to $\approx 161\text{ F g}^{-1}$.^[125] The LTO//KC21-900 LIC showed an energy density of $\approx 80\text{ Wh kg}^{-1}$ and 76% capacity retention after 10000 cycles. Madhavi et al. reported an AC derived from human hair (ACHH), which had a high specific surface area of $1116\text{ m}^2\text{ g}^{-1}$ and a relatively large average pore size of $50\text{--}100\text{ nm}$.^[126] The ACHH delivered a specific capacitance of $\approx 115\text{ F g}^{-1}$ at 100 mA g^{-1} . The LTO//ACHH LIC showed an energy density of 22.5 Wh kg^{-1} and an power density of 2 kW kg^{-1} . Shajumon et al. designed

an LIC by employing rice husk derived AC as cathode, which was obtained by chemically activating with KOH (RHDPC-KOH).^[127] The high specific surface area and favorable pore volume distribution are responsible for high capacity. A specific capacitance of 120 F g^{-1} was delivered at 2 A g^{-1} in $1\text{ M LiPF}_6/(\text{EC+DMC})$. The obtained energy density of LTO// RHDPC-KOH LIC was up to 45 Wh kg^{-1} even at $\approx 4.3\text{ kW kg}^{-1}$. The synergistic effect of the high ion intercalation anode coupling with high rate capacitive cathode was responsible for the improved electrochemical performance.

2.2.3. LTO (-)//Polymer Derived Porous Carbon (+)

Conventionally, porous AC is prepared by heat treatment of natural products followed by chemical activation techniques. However, these methods are not applicable to precise control of carbonaceous materials to obtain an ideal morphology with suitable structure, and physical/chemical features. Polymers can provide a possibility for precursor tunability with specially designated porous structure.^[128] Ogale et al. demonstrated an oligomer-salt-derived 3D porous carbon (ODC) cathode by means of pyrolysis of an oligomer salt tailored for molecular level activation (Figure 10).^[129] This strategy did not need chemical activating agents and the homogeneity of the material was guaranteed. The LTO//ODC LIC showed good rate capability and was able to deliver energy and power densities of $\approx 63\text{ Wh kg}^{-1}$ and $\approx 10\text{ kW kg}^{-1}$, respectively. Then, they also

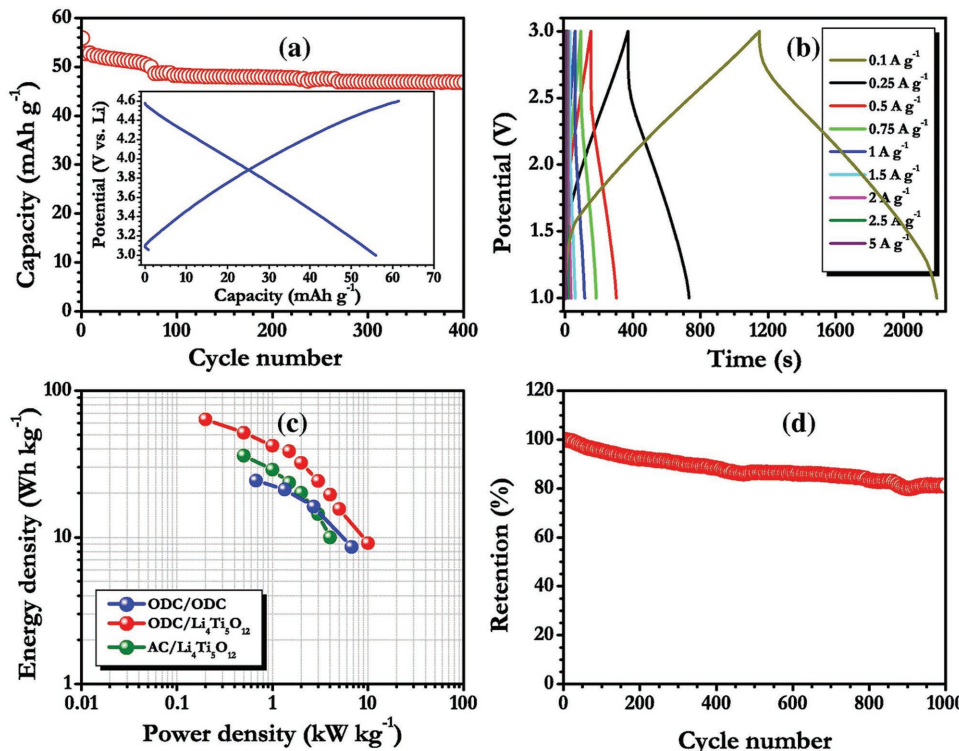


Figure 10. a) Cycle performance of ODC electrode between 3 and 4.6 V versus Li at 100 mA g^{-1} . Inset: charge–discharge profiles of ODC electrode, b) charge–discharge curves of LTO//ODC LIC between 1–3 V under varied current densities, c) Ragone plot of LTO//ODC and LTO//AC, and d) cycle performance of LTO//ODC LIC. Reproduced with permission.^[129] Copyright 2014, Elsevier.

developed a 3 D architected porous carbon (HSPC) using the poly(acrylamide-co-acrylic acid)potassium salt as starting material by was of a single step.^[130] The specific surface area and discharge capacitance of HSPC was up to $1490\text{ m}^2\text{ g}^{-1}$ and 123 F g^{-1} , respectively. The LTO//HSPC LIC could deliver an energy density of $\approx 55\text{ Wh kg}^{-1}$. Furthermore, Ogale et al. presented the first application of 3D carbon cuboids using a metal-organic framework (MOF-5).^[131] The specific surface area of the MOF derived carbon (MOF-DC) was as high as $2714\text{ m}^2\text{ g}^{-1}$. The MOF-DC electrode delivered a reversible capacity of 66 mAh g^{-1} at 150 mA g^{-1} . The LTO/MOF-DC LIC was able to deliver a maximum energy density of 65 Wh kg^{-1} . Kim et al. reported a novel bottom-up technique for the preparation of macrosized ($>500\text{ nm}$) graphene-like carbon using sp^2 carbon rich 1,2,4,5-benzene tetracarboxylic acid (BTCA) as a precursor.^[132] The method could produce defect free, pure high specific surface area, and sp^2 carbon-rich graphene. The specific surface area of the BTCA-derived carbon (BTCADC) was up to $2673\text{ m}^2\text{ g}^{-1}$ from $960\text{ m}^2\text{ g}^{-1}$ by chemical activation (A-BTCADC). The discharge capacities BTCADC and A-BTCADC electrodes are 48 mAh g^{-1} and 74 mAh g^{-1} , respectively. The LTO//A-BTCADC LIC showed an energy density of 63.5 Wh kg^{-1} with 97% capacity retention at 2 A g^{-1} up to 6000 cycles.

2.3. H-Ti-O Compounds (-)//Porous Carbon (+)

$\text{H}_2\text{Ti}_{12}\text{O}_{25}$ (HTO) is one of derivative of alkali titanium oxides by substituting the alkali element for H. Recently, much attention had been paid for its application in LIB anode.^[133,134] Due to its tunnel structures, HTO compounds exhibit good cycle stability, rate capability. HTO also shows much superior capacity ($\approx 236\text{ mAh g}^{-1}$) properties over LTO. So, it appears to be an attractive anode material for LICs.^[135,136] Many methods had been applied to enhance the electrochemical performance of HTO, including doping with metal ions and coating with conductive materials, etc.^[137] In this respect, Lee's group carried out a series of research work and made great achievements.^[138-143] They first prepared HTO by soft-chemical method in combination with ion exchange method.^[138] The energy density of cylindrical HTO//AC LIC reached to 35 Wh kg^{-1} at 179 W kg^{-1} . In order to promote the electrochemical properties of HTO, they also reported a thin film of AlPO_4 (2.25 nm, equal to 3 wt%) modified HTO.^[139] The proper coating of AlPO_4 on HTO was beneficial for suppression of side reactions at the electrode surface. The swelling phenomenon of the cylindrical LIC caused by gassing was markedly suppressed. Furthermore, AlPO_4 also worked as a bridge for the transfer of lithium ions and electrons between electrode and electrolyte. The LIC using 3 wt% AlPO_4 modified HTO anode showed an energy density of 41.1 Wh kg^{-1} at 194.1 W kg^{-1} with 94.1% capacity retention after 1000 cycles at a current rate of 3.0 A g^{-1} . Then, they also developed a carbon coated HTO compounds. The 4.5 wt% carbon-coated HTO showed an energy density of 38.8 Wh kg^{-1} at 5439.8 W kg^{-1} .^[140] Recently, AlPO_4 -carbon dual coated HTO anode (D-HTO) and AlPO_4 -carbon hybrid coated HTO (H-HTO) were further investigated by Lee's group.^[142] D-HTO

consisted of an inner carbon layer of 3.5 nm and outer AlPO_4 layer of 3.5 nm and delivered a discharge capacity of 257 mAh g^{-1} . The D-HTO//AC LIC showed the extraordinary capacity retention of 90.4% after 5000 cycles without a noticeable decrease, attributing to the tightly attached inner carbon layer and the strong P-O bond of outer AlPO_4 layer, which could effectively inhibit the HF attack under harsh condition and during cycling (Figure 11). The energy density of D-HTO//AC LIC was $\approx 16.9\text{ Wh kg}^{-1}$ at $\approx 19.7\text{ kW kg}^{-1}$, much better than the pristine HTO, carbon coated HTO (C-HTO), AlPO_4 coated HTO (A-HTO) and AlPO_4 -carbon hybrid coated HTO (H-HTO) based LICs. At the same time, they also prepared Nb-doped HTO ($\text{H}_2\text{Ti}_{12-x}\text{Nb}_x\text{O}_{25}$ ($0 \leq x \leq 0.6$)) anode with improved electronic conductivity and Li^+ diffusion,^[142] binary HTO-LTO with outstanding cycleability derived from LTO and excellent rate ability derived from HTO.^[143]

3. Carbon (-)//Porous Carbon (+) LICs

3.1. Graphite (-)//Porous Carbon (+)

One of the disadvantages of LTO-based LIC is that the voltage is greatly limited because the Li^+ intercalation/deintercalation plateau of LTO anode is 1.55 V versus Li^+/Li . Graphite is one of particularly attractive carbon materials for LIB anode because its Li^+ intercalation/deintercalation potential is located at $\approx 0.1\text{ V}$ versus Li^+/Li , high capacity (372 mAh g^{-1} for LiC_6 stoichiometry).^[144] Therefore, an LIC using graphite as anode and high specific surface area porous carbon as cathode will show greater energy storage capacity than conventional EDLC and LTO-based LIC.

Back to 2008, Béguin et al. investigated the graphite/AC LIC system.^[145] In this work, commercial available graphite and AC were used as anode and cathode, respectively. When the electrode weight of graphite to AC was 1:1, the best compromise between energy and power was reached. In order to decrease the potential of the graphite anode, "formation cycles" of the LIC was applied, as shown in Figure 12. Afterward the potential of the graphite anode maintained at 0.1 V versus Li^+/Li , which ensured the LIC with a stable cycle performance. The

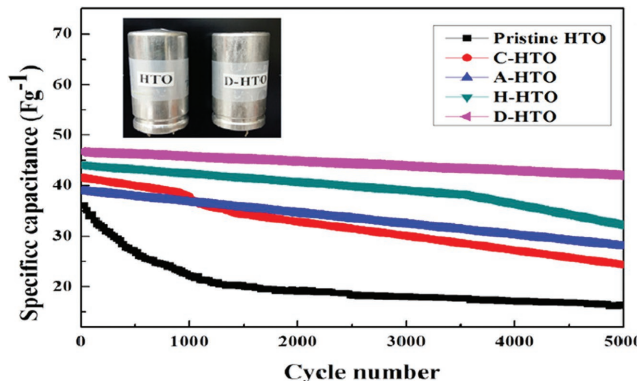


Figure 11. Cycling performance of the LICs using pristine and surface-modified HTO. Reproduced with permission.^[141] Copyright 2016, Elsevier.

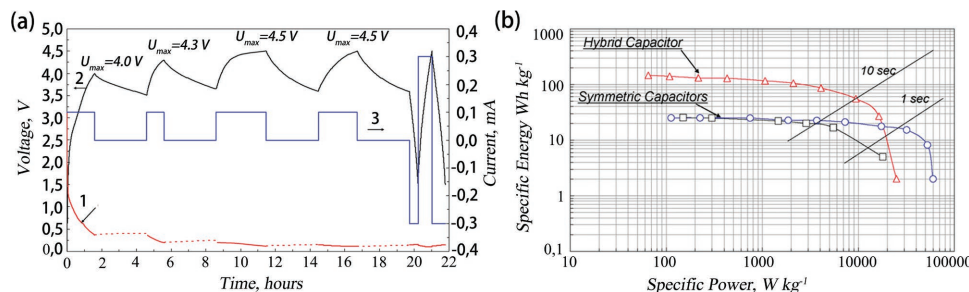


Figure 12. a) Charge–discharge curves (2) and current profiles (3) of the graphite/AC LIC during formation cycles at C/20. Curve (1) represents the potential variation of the graphite anode, whereas the dotted line stands for the relaxation process. $m_{\text{AC}}, m_{\text{graphite}} = 1:1$. b) Ragone plot of graphite/AC LIC (Δ) in 1 M LiPF₆/EC-DMC and for the symmetric capacitors in 1 M LiPF₆/EC-DMC (\square) and 1 M Et₄NBF₄/AN (\circ). Reproduced with permission.^[145] Copyright 2008, Elsevier.

energy densities were up to 103.8 Wh kg⁻¹ while keeping a very good cycleability with 85% capacity retention after 10 000 cycles.

The intercalation kinetics of lithium ion into graphite anode is much more sluggish than physical adsorption of anion onto high specific surface area AC cathode, so the rate capability is limited the graphite anode. Reducing graphite particle size could show good C-rate capability due to the shortened ion diffusion length. However, it was also accompanied by an increase in irreversible capacity loss caused by the increased electrode/electrolyte interface.^[146] It was reported that ball milling could decrease the size of graphite materials and improve the rate capability.^[147] Hard carbon coating on natural graphite was an effective method.^[148] Modification the morphology and surface characteristics of graphite by hydrogen peroxide treatment could increase the exposed edge planes and generate more stable solid-electrolyte interphase layers, which facilitate substantially power and cycling performance of the graphite anodes.^[149] Nitrogen-doped carbonized polyimide microspheres (CPIMS) with porous structure showed excellent capacity property and

rate capability. The CPIMS//AC LIC could show an energy density of 13.1 Wh kg⁻¹ at 6.94 kW kg⁻¹ on the basis of both electrode. 97.1% of the initial capacity was retained even after 5000 cycles at 0.5 A g⁻¹.^[150] Based on the similar idea, Sun et al. also developed an N-rich carbon spheres (NRCS, which possessed high specific surface area (1560 m² g⁻¹), uniform mesopore (10–15 nm), and high level of N-doping (14.51%), which enabled excellent lithium storage properties in relation to capacity, rate capability and cycleability.^[151] When NRCS//AC LIC was worked at 2.0–4.5 V, 40.4 Wh kg⁻¹ could be obtained at 10.8 kW kg⁻¹. Just recently, Zhang et al. fabricated a novel LIC using nitrogen-doped porous carbon microsphere (NPCM) anode and activated NPCM (NPCM-A) as cathode (Figure 13).^[128] The porous NPCM anode was beneficial for fast ion diffusion and intercalation and the high specific surface area NPCM-A cathode facilitated ion accumulation. The assembled NPCM (−)//NPCM-A (+) LIC could retain 48.2 Wh kg⁻¹ at 15 kW kg⁻¹.

On the other hand, many efforts were also made to promote the electrical conductivity and capacity of AC cathode. In 1 M LiPF₆/(EC+EMC+DMC) electrolyte, copper-coated AC cathode

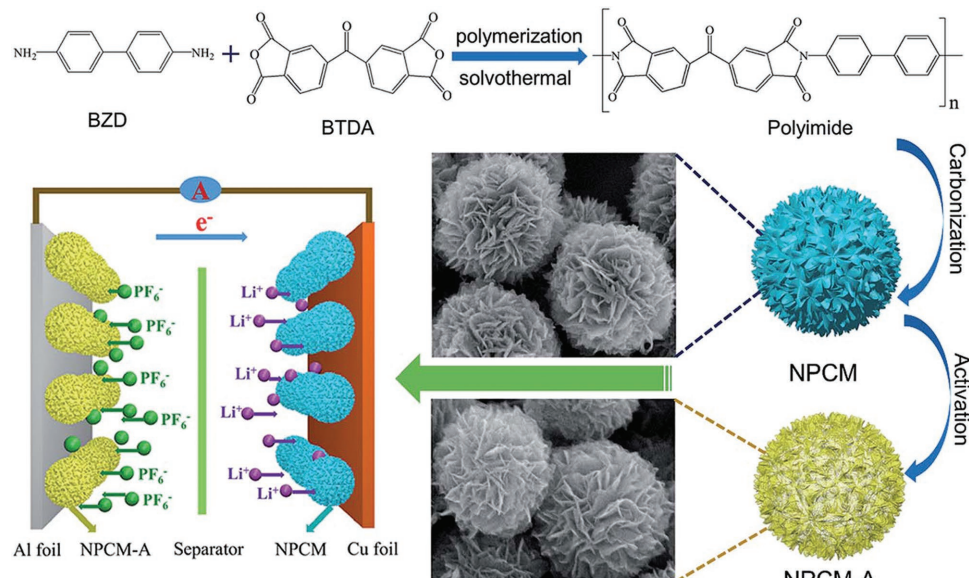


Figure 13. Schematic diagram of the preparation of NPCM anode and NPCM-A cathode and the charge storage mechanism. Reproduced with permission.^[128] Copyright 2017, Royal Society of Chemistry.

could deliver a specific capacitance of 59.25 F g^{-1} even at 100 C , better than that of pure AC electrode.^[152] Guo et al. demonstrated a sisal fiber AC (SFAC), which showed a moderate specific capacitance of 103 F g^{-1} at 0.1 A g^{-1} and superior cycle performance with 88% capacity retention after 5000 cycles at 1 A g^{-1} .^[153] The MCMB//SFAC LIC delivered an energy density of 41 Wh kg^{-1} even at 5.718 kW kg^{-1} .

3.2. Hard Carbon (−)//Porous Carbon (+)

Generally, hard carbon (HC) is prepared by heat treatment of polymer or biomass material at $\approx 1000 \text{ }^{\circ}\text{C}$ and shows better rate capability and more excellent cycleability than graphite. By virtue of these merits, it is a good choice for high power LIC application.^[154] Zheng et al. investigated various carbon materials for use as the negative electrodes in LICs including HC, soft carbon (SC) and graphite. Among all of these carbon materials, the LIC with HC anode exhibited the best power performance.^[155] The HC//AC and SC//AC LICs displayed better cycleability than that of graphite//AC LIC. After 100 000 cycles, the HC//AC LIC maintained a high discharge capacity retention of 85%.

Since the capacity of the AC cathode is much lower than that of the HC anode, in order to obtain higher energy density, the capacity of AC cathode must be promoted. Aida et al. extended the cell voltage of HC//AC LIC to 4.4 V (conventionally 3.8 V). It was interesting that when the AC cathode was $\geq 4.23 \text{ V}$ versus Li^+/Li : the higher the AC cathode, the greater the decline in the capacity of HC anode. A thin film of LiF was detected on HC anode, which was caused by the decomposition of PF_6^- at the AC cathode (Figure 14a). When an Li metal foil was placed between the cathode and anode, the HF was trapped on the Li metal, then the cycle durability of the HC anode was remarkably improved even the voltage reached to 4.4 V .^[156,157] They also reported a so-called “Nanogate Carbon” positive electrode, which was a graphitic carbon activated by KOH (i.e., KOH-activated SC).^[158] Such “Nanogate Carbon” had low specific capacitance because of its low specific surface area before charging. Nevertheless, after an “electrochemical activation” process by the first charging at potential above 4 V versus Li^+/Li in $\text{LiPF}_6/(EC+DMC)$, the capacity of KOH-activated SC ($3.0\text{--}4.7 \text{ V}$ vs Li^+/Li) increased to about 3 times higher than that of the

conventional AC ($3.0\text{--}4.0 \text{ V}$ vs Li^+/Li). The KOH-activated SC (+)//nongraphitizable carbon (−) LIC showed fascinating energy and power densities of 145.1 Wh kg^{-1} and 15.1 kW kg^{-1} , respectively.

In subsequent work of Zheng's group, they continued to develop advanced HC//AC LICs technologies. They placed a stabilized lithium metal powder (SLMP) onto the surface of the HC anode, which could compensate the electrolyte consumption and achieve much higher energy density.^[159] Moreover, in order to ensure the cycle stability and safety, the upper potential of AC cathode should be lower than 4.4 V versus Li^+/Li ; while the lower limit potential of HC anode should be higher than 0.1 V versus Li^+/Li . As far as an LIC was concerned, the upper potential of cathode was depended on the maximum charge voltage to the cell, while the lower limit potential of anode was dictated to by the mass ratio of cathode to anode.^[160] They optimized the cathode configuration, lithium loading on anode and the type of separator.^[161] When PTFE was chosen as binder and the mass ratio of SLMP to HC was 1:7, the energy density of LIC pouch cell could reach to 22 Wh g^{-1} . A long cycle life with energy retention of 94% after 10000 cycles was obtained. The mass loadings of SLMP on HC cathode also influenced the IR voltage drop during charge and discharge processes.^[162] The HC-lithium stripes//AC laminate cell could exhibit an energy density of 14 Wh kg^{-1} and a power density of 6 kW kg^{-1} . The cycle life was up to 50 000 cycles under 125 C rate.^[163] In order to improve the electrochemical performance of HC//AC LICs under high temperature and high voltage stress, Zheng found that 1% TMSP additive in EC+DMC electrolyte could retain 70.5% of the initial performance after floating at 3.8 V for $\approx 1200 \text{ h}$ at 65°C (Figure 14b).^[31]

Ma's group investigated the capacity fading behaviors of AC//HC based LIC pouch cells by monitoring the anode potential swings and the internal resistance changes.^[164] The capacity decay at high rate was a kinetic behavior caused by insufficient intercalation/deintercalation in fast faradaic process. The main reasons for the capacity decay upon cycling were attributed to the increase of internal resistance and the Li^+ consumption. Shi's group investigated the electrochemical performance of different kinds of HC materials in LIC. In comparison with the spherical HC, the irregular HC showed a distinct Li^+ intercalation plateau, which resulted in a lower voltage range than spherical HC based LIC.^[165]

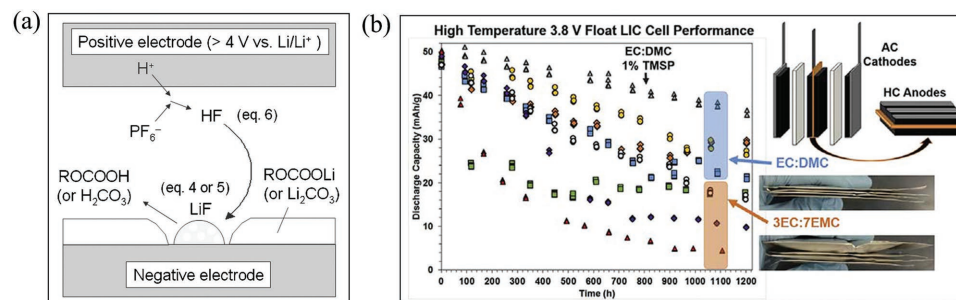


Figure 14. a) Probable diagram of LiF generation at high voltage LIC. Reproduced with permission.^[156] Copyright 2007, The Electrochemical Society. b) A schematic diagram of an HC//AC LIC configuration and the high temperature 3.8 V float LIC cell performance with 1% TMSP addition in $1 \text{ M LiPF}_6/(EC:DMC = 3:7 \text{ in mass ratio})$. Reproduced with permission.^[31] Copyright 2018, Elsevier.

3.3. Soft Carbon (-)//Porous Carbon (+)

The soft carbon (SC), which is heat-treated at ≈ 1000 °C, shows excellent characteristics in terms of high-rate charge/discharge performance and cycleability.^[166] Balducci et al. systematically investigated the influence of the structural properties of carbonaceous materials on electrochemical behavior of LIC.^[167] They found that the Li⁺ intercalation into graphite anode was limited when a new Li⁺ intercalation stage was reached; while in SC the Li⁺ intercalation did not show serious decline over the past potential range. Such different structural properties had deep influence on the cycleability during the high rates charge/discharge. When a current density equal to 15 C was applied on LIC, the SC//AC LIC delivered 35% energy higher than the graphite//AC LIC. SC seems to be more appropriate for LICs. Then, they investigated the electrochemical performance of the SC anode in propylene carbonate-based electrolytes.^[168] Even over 10000 cycles, the SC anode could maintain 80 mAh g⁻¹ at 5 C. After a proper prelithiation process, the SC//AC LIC showed an energy density of 21.7 Wh kg⁻¹ and power density of 4.1 kW kg⁻¹. When 1 M LiPF₆/(EC+DMC) was used as the electrolyte changed, an energy density of 48 Wh kg⁻¹ at 9 kW kg⁻¹ was delivered at the maximum operative voltage of 4 V.^[169] In order to enhance the rate capability, strategies by mixing of AC with pitch^[170] and incorporation of conductive polymer (PEDOT-PSS) into SC were also studied, allowing a faster lithium ion intercalation and diffusion.^[171]

4. Silicon-Based Composites (-)//Porous Carbon (+) LICs

Silicon has been widely investigated as a potential anode material in LIBs, by virtue of its low Li insertion/extraction potential (0.3–0.6 V vs Li⁺/Li) and high specific capacity over graphite material (theoretical value: 4200 mAh g⁻¹, crystalline Si; 3800 mAh g⁻¹, amorphous Si).^[172] However, the poor stability of bulk Si materials limits its application caused by the large volume expansion ($>300\%$) during lithiation. Nanostructuring and carbon coating are effective strategies to alleviate this disadvantage. The reports of Si-based anode in LICs are few in number. In 2009, Konno et al. synthesized an Si-C-O glass-like compound (a-SiCO) anode.^[51] Because of the high irreversible during the first lithiation and far excessive capacity over AC

cathode, the a-SiCO anode should be prelithiated by appropriate short-circuiting. The results showed that the cycle performance of LIC in LiBF₄/PC was better but the capacitance was smaller than in LiClO₄/(EC+DEC) electrolyte. In 2016, Zhang et al. demonstrated a high specific surface area AC derived from egg white.^[173] The reversible capacitance of the egg white based AC was 184 F g⁻¹ (128 mAh g⁻¹) in 1.2 M LiPF₆/(EC+DEC+DMC) as electrolyte at 0.4 A g⁻¹ in the voltage range of 2.0–4.5 V. A capacitance of 56 F g⁻¹ (39 mAh g⁻¹) could also be obtained even at 12.8 A g⁻¹ (128 C), due to a synergy of the abundant porous structure, high degree of graphitization and oxygen functional group. When it was paired with Si-C nanocomposite anode, the Si-C//AC LIC delivered an energy density of 147 Wh kg⁻¹ at 29893 W kg⁻¹ at 2.0–4.5 V. Recently, Tuan et al. developed a light and binder-free bilayer fabric electrode composed of Si nanowires (SiNWs) and Cu nanowires (CuNWs) (Figure 15).^[174] The Si/Cu bilayer fabric electrode could offer a high surface area for electrolyte accession, an excellent electrical conductivity, and a strong tolerance for volume change and improve the electrochemical performances toward the top-right region in Ragone plot. The Si/Cu bilayer fabric (-)//AC (+) LIC could maintain an ultrahigh energy density of 43 Wh kg⁻¹ even at 99 kW kg⁻¹.

5. Graphene-Based LICs

Due to the low capacities and poor electrical conductivity of AC cathode, the energy storage performance of LICs would be further improved by using other novel electrode materials with unique physical properties. Graphene is a kind of 2D allotrope of carbon-based materials. It has super high specific surface area (theoretically 2630 m² g⁻¹), good chemical stability and excellent electrical conductivity.^[175–178] These properties make graphene very attractive for use as electrodes in energy conversion and storage devices, especially in LICs. Most of the studies are focused on the modification of surface functional groups,^[179–181] porous-creating,^[182–184] and morphology control.^[185,186] Choi et al. used the urea-treated graphene to trigger an Li binding mechanism by virtue of its amide functional groups, leading to a promotion in energy density by 37.5% in comparison with those of using AC cathode. Consequently, a high energy density of 106 Wh kg_{total}⁻¹ and a power density of 4.2 kW kg_{total}⁻¹ were obtained.^[179] Kang et al. demonstrated a

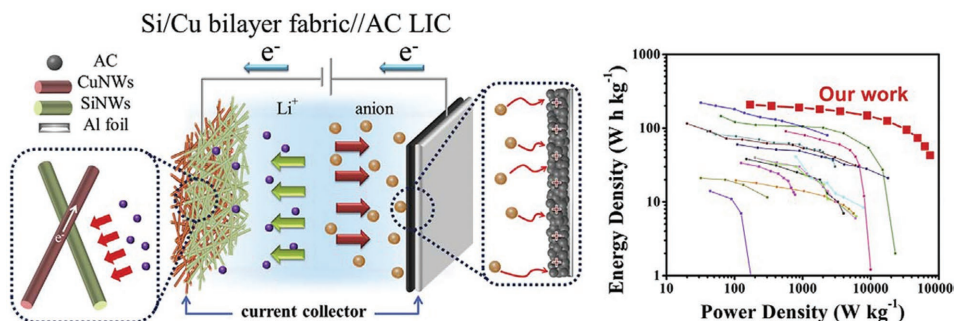


Figure 15. The schematic mechanism of the Si/Cu nanowires bilayer fabric//AC LIC and its Ragone plot in comparison with other reported LICs. Reproduced with permission.^[174] Copyright 2018, Elsevier.

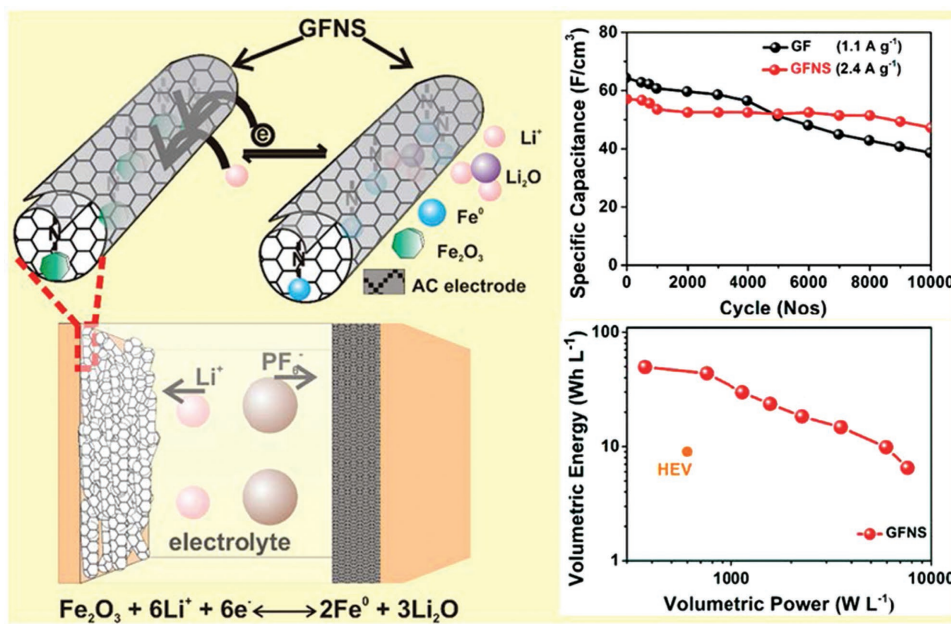


Figure 16. Schematic diagram of discharge/charge process, cycle performance and Ragone plots of the GFNS/AC cell. Reproduced with permission.^[189] Copyright 2017, American Chemical Society.

nitrogen-enriched mesoporous carbon nanospheres/graphene (N-GMCS) nanocomposite, which presented a combination of hierarchical porous structure, 3D conductive network, and high mass density.^[185] The LIC was formed by coupling with prelithiated microcrystalline graphite (PLMG) anode. It could deliver an energy density of 80 Wh kg⁻¹ and a power density of 352 kW kg⁻¹.

However, the functionalized graphene unavoidably went through rapid capacity degradation during cycling. Cheng et al. added lithium difluoro(oxalate)borate (LiODFB) into 1 M LiPF₆/ (EC+DMC).^[187] During galvanostatic discharge, the LiODFB was decomposed on the graphene and formed a protective layer. The protective layer could prevent the electrolyte from decomposition. As a result, the LIC displayed a small capacity fading of 0.011% per cycle. They further investigated the influence of pore size distribution, specific surface area and oxygen content of graphene material on the electrochemical stability of LICs in 5 V organic electrolyte. They found that the pore size distribution of graphene determined the electrochemical stability at 5 V. Graphene powders with small pores (smaller than 5 nm) were much more stable because of the restriction effect of small pores on electrolyte decomposition.^[188] Another problem of graphene based LICs is the low volumetric energy density due to the low packing density of graphene (<0.5 g cm⁻³).^[189] Correspondingly, the design and preparation of graphene with dense packing while without restacking and aggregation becomes a great challenge. During the past few years, graphene based electrode materials with the aim of improving volumetric energy density, including interlinked graphene nanosheets,^[190] electrochemically reduced graphene oxide hydrogels,^[191] 3D holey framework with hierarchical porous structure,^[192] pillarized graphene framework,^[193] etc., have been successfully developed. It should be mentioned that Lee's group proposed a supercapacitor with enhanced packing density and high

volumetric energy density using reduced graphene oxide (rGO) sheets scrolling and Fe₂O₃-wrapped nitrogen-doped rGO scrolls (GFNSs) as electrode materials (Figure 16).^[189] By synthesizing a doped scroll structure, the restacking of rGO sheets was well controlled. Meantime, the packing density of the electrode was highly improved. The fabricated cell exhibited an ultrahigh volumetric energy density of 49.66 Wh L⁻¹ and an excellent cycleability of over 10000 cycles.

6. Metal oxide (-)//Porous carbon (+) LICs

6.1. Titanium Oxide (-)//Porous Carbon (+)

TiO₂, by virtue of its excellent chemical stability, high theoretical capacity (TiO₂ (B): 335 mAh g⁻¹), nontoxicity, and low solubility in organic electrolyte solutions, have been widely investigated as a potential anode material for LIBs.^[194] Recently, as an intercalation host, TiO₂, instead of LTO, is also coupled with porous carbon cathode to form high performance LICs. Brousse et al. synthesized TiO₂ (B) by a solid-state reaction and hydrolysis. The TiO₂(B)//AC LIC could exhibit energy densities of 45–80 Wh kg⁻¹ with power densities of 240–420 W kg⁻¹.^[49] In order to solve the poor electronic conductivity and low ion diffusion problems, nanosized TiO₂ or its composite were developed, including TiO₂B nanowire,^[50] TiO₂-(reduced graphene oxide),^[195] TiO₂-B nanorods,^[196] TiO₂ nanobelt arrays,^[197] porous anatase TiO₂ nanoparticles,^[198] urchin-like TiO₂^[199] and porous TiO₂ hollow microspheres @graphene nanosheets,^[180] and so on. These nanostructured materials play important roles in lithium-intercalation kinetics, by virtue of their shortened diffusion lengths and increased specific surface area, which are important for fast charge/discharge of LIC. Thus the power capability between

the faradic anode and capacitive cathode could be well balanced, leading to higher energy densities even working at high power densities. The anatase TiO_2 -reduced graphene oxide//AC LIC achieved an energy density of 42 Wh kg⁻¹ at 0.8 kW kg⁻¹ at 1.0–3.0 V. Even at a 4 s rate, 8.9 Wh kg⁻¹ could also be obtained.^[195] Wang et al. developed a free-standing TiO_2 nanobelt arrays with a highly open structure as anode, which were grown perpendicular to Ti foil and avoided the use of conductive carbon/polymeric binder.^[197] Graphene hydrogels cathode could deliver more than 75% retention in the capacitance relative to 0.5 A g⁻¹. When TiO_2 nanobelt array//graphene hydrogel LIC worked at 0.0–3.8 V, 21 Wh kg⁻¹ was obtained at 19 kW kg⁻¹. Wu et al. developed a quasi-solid-state

LIC using porous TiO_2 hollow microspheres@graphene nanosheets as anode.^[200] The TiO_2 hollow microspheres were ≈450 nm in diameter, consisting of a large amount of the interconnected TiO_2 nanocrystals. Moreover, PVDF-HFP based gel polymer electrolyte was applied to substitute the conventional liquid electrolyte. The quasi-solid-state LIC by coupling the electrochemical-exfoliated graphene nanosheets cathode with the porous TiO_2 hollow microspheres@graphene nanosheets anode could deliver an energy density of 10 Wh kg⁻¹ at 2 kW kg⁻¹, as listed in Table 2.

TiP_2O_7 is another kind of titanium-based oxide used for lithium ion intercalation host in LIBs. There are a few reports on the use of TiP_2O_7 as LIC anode. Chowdari et al.

Table 2. The electrochemical performance of various LICs based on metal oxide anode.

System	Cathode	Anode	Voltage [V]	Power density [W kg ⁻¹]	Energy density [Wh kg ⁻¹]	Ref.
Titanium Oxide (-)//Porous carbon (+)	AC	TiO_2 (B)	1.2–3.2	240–420	45–80	[49]
	CNT	TiO_2 -B nanowire	0.0–2.8	/	12.5	[50]
	AC	TiO_2 -reduced graphene oxide)	1.0–3.0	800	42	[195]
	AC	TiO_2 -B nanorods	0.0–2.8	2800	23	[196]
	Graphene hydrogels	TiO_2 nanobelt arrays	0.0–3.8	19000	21	[197]
	AC	Porous anatase TiO_2	0.0–3.0	150	60.75	[198]
	AC	Urchin-like TiO_2	0.0–2.8	12224.3	10.1	[199]
	Graphene nanosheets	TiO_2 hollow microspheres@graphene	0.0–3.0	2000	10	[200]
	AC	nano- TiP_2O_7	0.0–3.0	371	13	[201]
	Graphene grass	3D ordered porous TiNb_2O_7 nanotubes	0.0–3.0	7500	34.5	[202]
Vanadium Oxide (-)//Porous carbon (+)	Carbon fiber	TiNb_2O_7 @carbon	0.8–3.2	5464	20	[203]
	AC	Intertwined CNT/ V_2O_5 nanowire	0.1–2.7	210	40	[205]
	AC	Graphene- V_2O_5 nanorod	0.0–2.7	1075.9	23.7	[206]
Iron Oxide (-)//Porous carbon (+)	AC	$\beta\text{-FeOOH}$	1.5–2.8	/	45	[207]
	MWNT	$\alpha\text{-Fe}_2\text{O}_3$ /MWNT	0.0–2.8	1000	50	[208]
	AC	$\alpha\text{-Fe}_2\text{O}_3$	0.0–3.4	/	90	[209]
	Nitrogen-doped hierarchical porous carbon	Fe_2O_3 @carbon	1.0–4.0	9200	31	[210]
	3D graphene	Fe_3O_4 @graphene	1.0–4.0	4600	65	[211]
Manganese oxide (-)//Porous carbon (+)	3D hierarchical porous N-doped carbon	MnO @graphene	1.0–4.0	25000	83.25	[212]
	AC	Spindle MnO	0.1–4.0	2608	220	[213]
	AC	Mesocrystal MnO cubes@carbon	0.1–4.0	2952	227	[214]
	AC	Mn_3O_4 octahedrons@graphene	1.5–4.0	≈648	≈142	[215]
	Graphene aerogels	T- Nb_2O_5 Nanowires@carbon Cloth	2.6–4.0	521.7	2.6	[216]
Niobium oxide (-)//Porous carbon (+)	AC	Nb_2O_5 @graphene	1.0–3.0	2900	29	[217]
	AC	Nb_2O_5 @carbon	1.0–3.5	16528	5	[218]
	AC	Nb_2O_5 quantum dots@MOF derived nitrogen-doped porous carbon	0.5–4.0	11250	22.4	[219]
	Biomass-derived carbon nanosheets	Flexible Nb_2O_5 nanowires/graphene film	1.0–4.0	14000	32	[220]
	Mesoporous carbon coated rGO	Mesoporous T- Nb_2O_5 nanospheres@graphene		25600	21	[221]
	AC	Nb_2O_5 /ordered mesoporous carbon	0.5–3.0	8750	24.4	[222]
	AC	T- Nb_2O_5 @carbon nanowires	1.0–3.5	85000	27	[223]

first developed a nanosized $\text{TiP}_2\text{O}_7/\text//\text{AC}$ LIC, showing a maximum energy density of 13 Wh kg^{-1} and power density of 371 W kg^{-1} .^[201] Zhang et al. developed a 3D ordered porous TiNb_2O_7 nanotubes (3D-O-P-TNO).^[202] the capacity of the TiNb_2O_7 half-cell still retained 116.6 mAh g^{-1} even at 30 C . The LIC, 3D-O-P-TNO//graphene grass LIC maintained an energy density of as much as 34.5 Wh kg^{-1} at 7.5 kW kg^{-1} at $0\text{--}3 \text{ V}$. Shen et al. also investigated the electrochemical properties of $\text{TiNb}_2\text{O}_7@\text{carbon microwires}/\text//\text{carbon fibers}$ LIC (20 Wh kg^{-1} at 5.464 kW kg^{-1}).^[203]

6.2. Vanadium Oxide (-)//Porous Carbon (+)

Layer-structured vanadium pentoxide (V_2O_5), owing to its high specific capacity ($\approx 300 \text{ mAh g}^{-1}$) and low cost, has been extensively studied as anode material in LIBs. Recently, it was also used as anode active material in LICs.^[204] However, the key challenges for V_2O_5 in LICs are the phase transition during lithium intercalation/deintercalation and poor electrical conductivity, which influence the power capability of LICs. Hybridizing nanostructured V_2O_5 with carbonaceous materials is an effective method to remedy these disadvantages. Intertwined CNT/ V_2O_5 nanowire nanocomposites^[205] and graphene- V_2O_5 nanorod composite^[206] are representatives. The incorporation of V_2O_5 with 1D CNT or 2D graphene conductive agents ensured fast and efficient electron transfer and collection. The nanosized profile is beneficial to maintain structural stability during repeatedly charge/discharge. The above two materials can deliver 23.7 Wh kg^{-1} at 1075.9 W kg^{-1} . The cycleability is also greatly improved.

6.3. Iron Oxide (-)//Porous Carbon (+)

In 2006, Xia et al. first investigated the electrochemical behaviors of nanostructured FeOOH as anode material in LIC.^[207] The $\text{FeOOH}/\text//\text{AC}$ LIC showed a capacity of 30 mAh g^{-1} at $1.5\text{--}2.8 \text{ V}$, corresponding to an energy density of 45 Wh kg^{-1} . Fe_3O_4 has been drawing great attention in LIB, due to its high capacity (924 mAh g^{-1}) and natural abundance. However, the poor rate capability and cycleability caused by severe aggregation and dramatic volume variation during Li^+ intercalation/deintercalation limit its application in high power LICs. By incorporation with carbon nanotube, the internal resistance and the ion diffusion behavior are highly improved.^[208] Carbon coating is also an effective way to promote the electrical conductivity and structure stability of Fe_3O_4 material.^[209,210] The carbon-coated $\text{Fe}_2\text{O}_3/\text//\text{nitrogen-doped hierarchical porous carbon}$ LIC system could deliver an energy density of 31 Wh kg^{-1} at 9.2 kW kg^{-1} .^[210] Graphene is also introduced to form an $\text{Fe}_3\text{O}_4/\text{graphene}$ nanocomposite.^[211] The graphene could inhibit the agglomeration of the Fe_3O_4 particles, control the size to nanoscale, create cross-linked channels and facilitate fast Li ion transport and electron transfer. The graphene acted as “elastic buffer” to alleviate the cracking of Fe_3O_4 nanoparticles and inhibited the volume variations during the cycling. The $\text{Fe}_3\text{O}_4\text//\text{3D graphene}$ LIC system exhibited an energy density 65 Wh kg^{-1} at 4.6 kW kg^{-1} .

6.4. Manganese Oxide (-)//Porous Carbon (+)

Until 2015, the work on the use of manganese oxide (MnO) based anode of LIC was reported.^[212] The problems, low conductivity, diffusion shortage and structural collapses, were well resolved by dispersing MnO nanocrystals ($\approx 5 \text{ nm}$) into the 3D graphene architecture. When it was incorporated with 3D hierarchical porous N-doped carbon cathode, the LIC could work in an encouraging potential range from 1 to 4 V and keep a super high capacity retention of $\approx 66\%$ even at 40 A g^{-1} . This LIC system achieved a very desirable energy density of 83.25 Wh kg^{-1} at 25 kW kg^{-1} . Cao et al. found that MnO nanoparticles with cationic vacancies and low degree of crystallinity could benefit phase transition and ion diffusion ($3.37 \times 10^{-13} \text{ cm}^2 \text{ s}^{-1}$).^[213] Moreover, the MnO nanoparticles encapsulated in 3D porous carbon could improve the electrical conductivity, offer ion diffusion channel. The $\text{MnO}/\text//\text{AC}$ LIC obtained energy and power densities of 220 Wh kg^{-1} and 2608 W kg^{-1} , respectively on the basis of active materials. The capacity retention was up to 95.3% after 3600 cycles at 5 A g^{-1} . Similarly, Cao et al. also synthesized mesocrystal MnO cubes containing considerable amount of Mn^{3+} ($\approx 11.8\%$), which was deemed to be the reason of the improvement of Li^+ diffusion coefficient.^[214] It had specific surface area of $74.3 \text{ m}^2 \text{ g}^{-1}$, appropriate carbon content of 11.7 wt\% and suitable particle size of 16 nm . As a result, the $\text{MnO-C}/\text//\text{AC}$ LIC showed an energy density of 227 Wh kg^{-1} and a power density of 2952 W kg^{-1} at $0.1\text{--}4.0 \text{ V}$. Another kind of manganese oxide, Mn_3O_4 , was also incorporated with few layer graphene to be served as anode of LIC.^[215] The $\text{Mn}_3\text{O}_4\text//\text{graphene}/\text//\text{AC}$ LIC showed a maximum energy density of 142 Wh kg^{-1} and 80% capacity retention after 9000 cycles, as listed in Table 2.

6.5. Niobium Oxide (-)//Porous Carbon (+)

A great challenge for the use of Nb_2O_5 as anode of LIC is the poor electron conductivity ($\approx 3.4 \times 10^{-6} \text{ S cm}^{-1}$ at 300 K).^[216] Combining Nb_2O_5 with conductive carbonaceous materials is a promising way to overcome this problem, including free-standing T- Nb_2O_5 nanowires@carbon cloth (2.6 Wh kg^{-1} at 521.7 W kg^{-1}),^[207] binder-free $\text{Nb}_2\text{O}_5@\text{graphene}$ (29 Wh kg^{-1} , 2.9 kW kg^{-1}),^[217] $\text{Nb}_2\text{O}_5@\text{carbon core-shell}$ nanocrystals (5 Wh kg^{-1} at $16.528 \text{ kW kg}^{-1}$),^[218] Nb_2O_5 quantum dots@MOF derived nitrogen-doped porous carbon (22.4 Wh kg^{-1} at 11.25 kW kg^{-1}),^[219] flexible Nb_2O_5 nanowires@graphene film (32 Wh kg^{-1} at 14 kW kg^{-1}),^[220] mesoporous T- Nb_2O_5 nanosphere@graphene (21 Wh kg^{-1} at 25.6 kW kg^{-1}),^[221] Nb_2O_5 nanoparticles@ordered mesoporous carbon matrix (24.4 Wh kg^{-1} at 8.75 kW kg^{-1}),^[222] and self-assembled orthorhombic phase niobium oxide@carbon nanowires (27.0 Wh kg^{-1} at 8.5 kW kg^{-1}), as listed in Table 2.^[223]

7. Graphite, HC, LTO, or AC (-)//LIB Cathode Material (+) LICs

As we all known, the rate capability of LIB is greatly restricted by the comparatively low kinetics of intercalation/deintercalation of lithium ions.^[224] AC is one kind of porous carbon

materials with high specific capacity, which can adsorb/desorbs ions and provide abundant ion diffusion channels. In view of such circumstance, a new type of LIC was developed by adding AC into LIB cathode or replacing graphite anode by AC anode, which can greatly compensate the shortcoming of power capability of LIB at the cost of decreasing energy density.^[225–227] Such kind of LICs can be classified into three types as follows.

7.1. Graphite or HC (−)/LIB Cathode Material-AC (+)

For this type LIC, MCMB//(LiFePO₄-AC),^[228] graphite//(LiNi_{0.5}Co_{0.2}Mn_{0.3}O₂-AC)^[229] and HC//(LiNi_{0.5}Co_{0.2}Mn_{0.3}O₂-AC)^[230] had been well investigated. The influence of the ratio of LIB cathode material to AC on the power density and energy density was systematically studied. It was found that the energy density was decreased with the increase of AC in the composite cathode, while the power capability was enhanced.^[229] Moreover, by virtue of the good rate capability of HC, the HC//(LiNi_{0.5}Co_{0.2}Mn_{0.3}O₂-AC) LIC delivered an energy density of 28.5 Wh kg⁻¹ even at 6.9 kW kg⁻¹. More than 98% the initial capacity was retained after 20000 cycles.^[230] Recently, Zheng also developed a kind of LIC consisting of LiNi_{0.5}Co_{0.2}Mn_{0.3}O₂-AC cathode and HC anode. The difference between this LIC and previous reports is the utilization of prelithiated HC anode. By controlling the amount of LiNi_{0.5}Co_{0.2}Mn_{0.3}O₂ in the cathode and prelithiation level, the energy density, power density and cycleability could reach to a good balance.^[231]

7.2. LTO (−)/LIB Cathode Material-AC (+)

Back in 2004, Amatucci et al. constructed a so-called “power-ion battery,” using an LiCoO₂-AC cathode and a nanostructured LTO anode, which could be fully charged in 3 min and achieve an energy density of 40 Wh kg⁻¹ and power density of 4 kW kg⁻¹.^[43] The power density was typical characteristic of LIC, much higher than that of the LIB. After that, LTO//(LiFePO₄-AC)^[232] and LTO//(LiMn₂O₄-AC)^[233] systems were also developed by Deng's group. They found that there existed six steps during charge/discharge due to different energy storage mechanisms (Figure 17). As shown in Figure 17a, the step B-C stood for the Li⁺ intercalation/deintercalation in LiFePO₄ and in LTO. The voltage variation of step C-D was linear with capacity, which was the characteristic charge process of adsorbing PF₆⁻ in AC and Li⁺ intercalation into LTO. Figure 17b,c stood for the typical LTO//LiFePO₄ battery and LTO//AC LIC charge/discharge curves. The similar charge/discharge profiles were presented at LTO//(LiMn₂O₄-AC) LIC system.^[233] The mass and volume energy densities of LTO//(LiMn₂O₄-AC) LIC reached to 16.47 Wh kg⁻¹ and 27.17 Wh L⁻¹, respectively, when the content of LiMn₂O₄ in composite cathode was up to 30 wt% in CC-CV mode.

Kötz et al. designed two kinds of systems, a serial and a parallel approach with two mass ratios of LIB materials over AC, as shown in Figure 18.^[234] The parallel hybridization of EDLC and LIB was superior to the serial approach for pulsed applications, improving the energy density of ECs and the power density of LIBs and providing moderately high specific energy and power. Although the serial hybrid could slightly improve the energy density, the

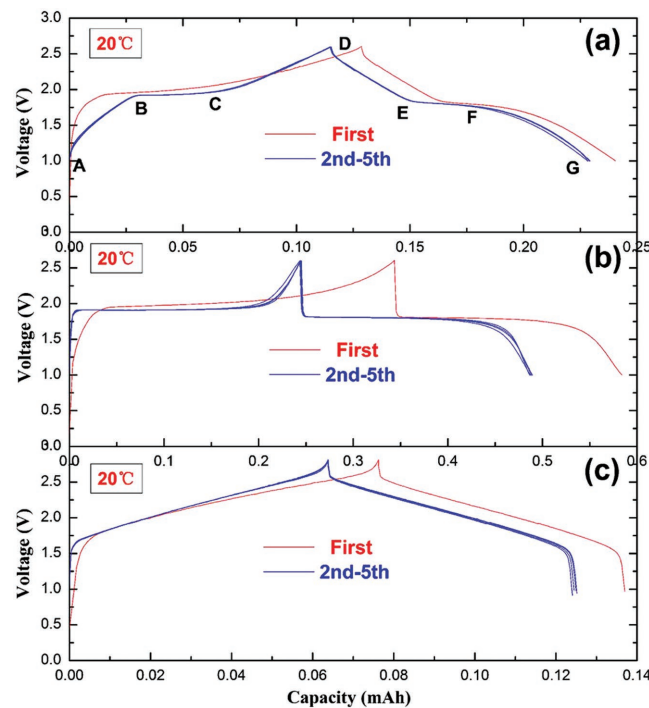


Figure 17. Charge/discharge cycle of a) the AC//(LiFePO₄-AC) LIC, b) the LTO//LiFePO₄ battery, and c) the LTO//AC LIC. Reproduced with permission.^[232] Copyright 2007, The Electrochemical Society.

power density was similar to the power of the battery. Inspired by this finding, LiFePO₄//(LTO-porous graphitic carbons) and (LiMn₂O₄-AC)//(LTO-AC) systems were also studied.^[30,235]

7.3. AC (−)/LIB Cathode Materials (+)

The merits of graphite as anode of LICs is its low intercalation potential, which can lead to a high energy density. However, the formation of lithium dendrites and the poor rate capability at high current limit its use as anode materials in LIC. Fortunately, ITO can effectively inhibit such problem, but its high lithium intercalation/deintercalation potential (1.55 V vs Li⁺/Li) restricts the voltage of LIC at low level. If AC is used as anode and store charges through physical ion adsorption/desorption mechanisms, the above problems can be well resolved. Recently, AC//LiNi_{0.5}Mn_{1.5}O₄,^[48,236–238] AC//LiMn₂O₄,^[239] AC//Li[Ni_{1/3}Co_{1/3}Mn_{1/3}]O₂,^[240] AC//LiFePO₄,^[241] and other types, such as AC//Li₂MnSiO₄,^[242] AC//Li(Mn_{1/3}Ni_{1/3}Fe_{1/3})O₂,^[243] and AC//Li₂CoPO₄F^[244] LIC systems had been extensively investigated. Especially, carbon-coated AC//Li₂MnSiO₄, AC//Li(Mn_{1/3}Ni_{1/3}Fe_{1/3})O₂-PANI based LICs could deliver energy densities of 37 and 49 Wh kg⁻¹ at power density of 1.5 and 1 kW kg⁻¹, respectively.^[242,243]

8. Polymer Cathode LICs

The main limitation of LTO//AC LICs is the decomposition of the electrolyte at AC electrode, leading to the similar

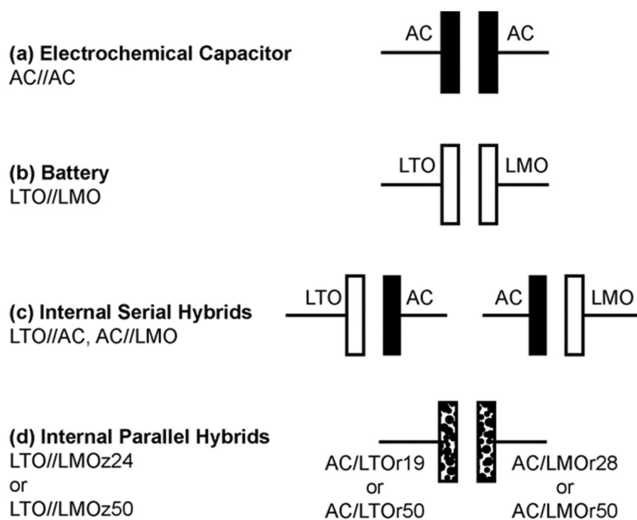


Figure 18. A schematic diagram of the various systems based on the electrode materials AC, LTO, and LMO and on the different bimaterial electrodes. a) Electrochemical capacitors, b) battery, c) two internal serial hybrids having the battery material in the negative or in the positive electrode, respectively, and d) internal parallel hybrids using different mass ratio composite electrodes, respectively. Reproduced with permission.^[234] Copyright 2011, Elsevier.

self-discharge problem as EDLCs. Moreover, the specific capacity and electrical conductivity of AC are relative low, which restrict the energy density and power density.^[245] In 2001, accompanied with the design of LTO//AC LICs by Amatucci et al., they also developed a kind of LIC by replacing the AC cathode by a pseudocapacitive organoredox cathode.^[246] Such pseudocapacitive organoredox cathode material could not only store/release energy by adsorption/desorption, but also utilize the *p*-doping of the polymer cathode, generating a higher average output voltage and reducing gassing and self-discharge of the LIC devices. Thus, better charge retention, higher energy and power density could be expected. After a series of optimizing work being done, a packaged LTO//poly(fluorophenylthiophene) LIC was made with various electrode thickness using 2 M LiBF₄ in CH₃CN as electrolyte. For thick electrodes, 20 Wh kg⁻¹ at 1 kW kg⁻¹ were obtained. For thinner electrodes, 16 Wh kg⁻¹ at 2.5 kW kg⁻¹ were achieved. Moreover, self-discharge was much lower than that of EDLCs or LTO//AC LICs. It should be noted that the cycle performance was somewhat unsatisfactory. In 2004, Pasquier et al. replaced the poly(fluorophenylthiophene) cathode with poly(methyl)thiophene (PMeT).^[247] Improved cycle performance was displayed due to a high molecular weight polymer free of oligomers and impurities. Based on the similar mechanisms, Lee' group also developed an LiMnBO₃ nanobead// polyaniline-nanofiber LIC.^[248,249] In light of excellent intercalation/deintercalation property of LiMnBO₃ nanobead and highly reversible doping/dedoping behavior and good electrical conductivity of polyaniline-nanofiber, a reversible specific capacitance of 125 F g⁻¹ was delivered at 1 A g⁻¹ at 0–3 V. Even at 2.25 A g⁻¹, the LIC could also deliver a specific capacitance of 55 F g⁻¹ and still retained 94% of the initial capacitance after 30000 cycles. More importantly, encouraging energy and power densities of 42 Wh kg⁻¹ and 5.35 kW kg⁻¹, respectively, were achieved.

9. Symmetrical LICs

Symmetrical LIC is a kind of energy storage device which use the same active materials both on cathode and anode in organic lithium ion electrolyte, which is different to EDLCs in quaternary ammonium salt based electrolyte.^[250–252] Sometimes, in order to keep a stable intercalation/deintercalation, extra lithium source in one of electrode is needed to provide lithium ions during repeated cycles. In 2009, Kim et al. proposed a symmetrical LIC using two non-prelithiated MnO₂-CNTs as cathode and anode.^[253] The stabilized lithium metal powder (SLMP) was placed at cathode. Thus, a pure MnO₂-CNT-SLMP//MnO₂-CNT LIC was obtained. During the first charge, lithium ions were extracted from cathode (SLMP), which could provide extra lithium ions by preventing the depletion of ions during charge and was beneficial for improving rate capability. The calculated energy density was 42 Wh kg⁻¹ at 1.8 kW kg⁻¹ at 0–3 V.

During the past few years, Cui's group developed mesoporous TiN microspheres^[53] and a series of graphene nanocomposites, including graphene-TiN,^[54] graphene/MoO₂,^[56] graphene/MoN^[55] and NbN/nitrogen doped graphene (NbN/NG).^[57] Lithium foil was served as lithium ion resources in all of these systems. The graphene provided good electrical conductivity and abundant ion adsorption sites. The lithium predoping method could offer a stable and constant potential and was favorable for cycleability. Moreover, during charge/discharge, Li₃N, a kind of fast ion conductor, would be formed onto the interface of electrode,^[254,255] which was beneficial for the decrease of interfacial resistance. It should be mentioned that the NbN/NG-based LIC could deliver a high energy density of 122.7 Wh kg⁻¹, a power density of 2 kW kg⁻¹, and maintained 81.7% capacity retention after 1000 cycles, when the mass ratio of NG in NbN/NG was 50%, as showed in Figure 19.

Pure carbon based symmetrical LIC was also extensively investigated, including microporous carbide derived carbon,^[256] AC-CNT composite^[257] and graphene-carbon nanotube carpets (G-CNTs).^[258] It was worth mentioning that Tour et al. reported homogeneous growth of single to few-walled carbon nanotube carpets from 3D graphene substrates, using Fe₃O₄/AlO_x nanoparticles as catalysts, as shown in Figure 20.^[258] The seamless connection between G and CNT and porous structure lead to fast electron transfer and ion diffusion. The G-CNTs were used directly as active material of anode and cathode free of binder, extraordinary specific capacities of ≈1250 mAh g⁻¹ at anodes and ≈100 mAh g⁻¹ at cathodes were obtained. Moreover, by virtue of the excellent electrochemical conductive network, even at 20.5 kW kg⁻¹, an encouraging energy density of 29 Wh kg⁻¹ was delivered.

10. Other LICs

10.1. LICs with Gel-Based Electrolytes

Generally, with regard to the LICs that are extensively studied in the lab or currently available in the market, liquid electrolytes including flammable organic solvents are used, such as linear carbonates or cyclic carbonates. The safety issues

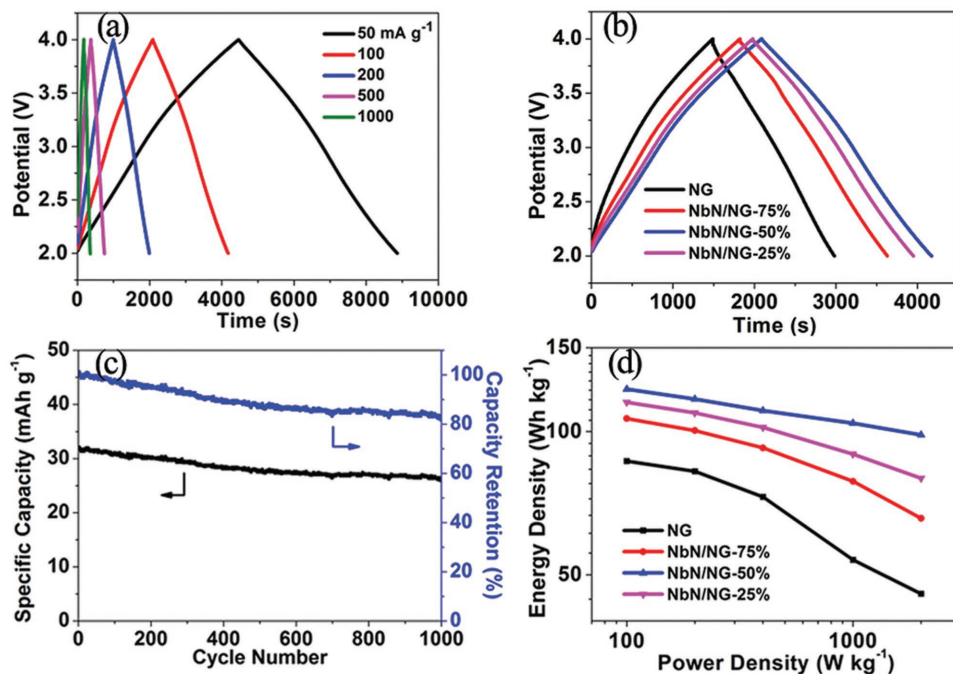


Figure 19. a) Charge–discharge profiles of LICS at various current densities using NbN/NG-50% as anode, b) charge–discharge profiles of LICs with NG and NbN/NG-X (X is the mass ratio of NG in NbN/NG) at 0.1 A g^{-1} , c) cycle performance of NbN/NG-50% based LIC at 0.5 A g^{-1} , and d) Ragone plots. Reproduced with permission.^[57] Copyright 2015, Wiley-VCH.

in relation to electrolyte leakage, short circuit, etc., are unavoidable. Gel, solid or quasi-solid electrolytes may well compensate these disadvantages.^[259,260] Tsai et al. prepared a minicapacitors with and without a PVdF-HFP gel polymer in the LiPF₆-based organic electrolytes.^[261] When the LIC operated in a low voltage window (2.0 or 2.5 V), the energy and power in cycling were stable both in LiPF₆/(EC+DMC) and PVdF-HFP gel electrolyte. However, when the voltage window extended to a higher level (2.5 or 4.0 V), high irreversible capacity or bad cycle performance caused by the electrolyte reduction at the negative electrode were presented in LiPF₆/(EC+DMC) electrolyte. While the addition of PVdF-HFP polymer could greatly decrease the electrolyte decomposition, improve the cycle stability (almost $\approx 20\%$ higher than LiPF₆/(EC+DMC) electrolyte after 10000 cycles) and enhance the coulombic

efficiency. Afterward, a ladder-like structured poly(ethylene oxide)-co-methacryloxypropyl)silsesquioxane (PEO-SQ) hybrid-type polymer gelator was introduced to prepare hybrid ionogel electrolytes by Koo et al.^[262] The inorganic ladder-like polysilsesquioxane backbone was beneficial to the thermal and electrochemical stability. Meanwhile, dual organic pendant groups consisting of free-dangling PEO chains and unsaturated methacryloxypropyl groups were good for lithium ion dissociation and thermal curing, respectively. When 1 m LiTFSI in *N*-butyl-*N*-methylpyrrolidinium bis(trifluoromethylsulfonyl)imide (BMPTFSI) ionic liquid was coupled with 5wt% of PEO-SQ, higher thermal stability ($\approx 400^\circ\text{C}$), larger ionic conductivity, and more excellent rate capability and cycleability were obtained, in comparison with those of pure ionic liquid electrolyte and organic-based crosslinkers without PEO groups. Gel-based LICs have not yet received much attention. Much effort should be made in the future. It is an interesting research area, as such devices with high safety are very suitable for hybrid or fully electronic vehicle applications.

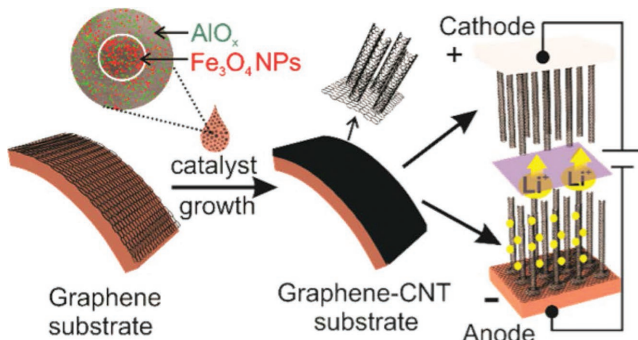


Figure 20. Scheme for the growth of G-CNT hybrid materials. Reproduced with permission.^[258] Copyright 2017, American Chemical Society.

10.2. Transition-Metal Carbide Materials (–)//Porous Carbon (+) LICs

In 2016, Yan et al. designed and a high energy LIC by coupling a pyridine-derived hierarchical porous nitrogen-doped carbon (PHPNC) cathode and a 3D interconnected titanium carbide (TiC) nanoparticle chain anode.^[263] The 3D TiC was prepared using carbothermal reaction of graphene/TiO₂ hybrid aerogels. The 3D TiC half-cell test indicated that an extraordinary high specific capacity of 137 mAh g^{-1} was obtained under

20 A g^{-1} . More encouragingly, the prepared PHPNC material delivered $\approx 42.3 \text{ mAh g}^{-1}$ at 30 A g^{-1} . Both of them exhibited an excellent rate capability. The TiC//PHPNC LIC showed a superior energy density of 35.6 Wh kg^{-1} even at 67.5 kW kg^{-1} . The intrinsic kinetics and capacity mismatch in an integrated system was well resolved. For TiC, pseudocapacitive with a wide working potential of $0.005\text{--}3 \text{ V}$ versus Li^+/Li , 3D interconnected nanoparticle chains and good electrical conductivity were the main reason for the good electrochemical performance.

Another new family of 2D transition metal carbides known as “MXenes,” have also demonstrated good lithium storage capabilities and been systematically studied by Gogotsi group.^[264,265] MXene-based electrodes are conventionally operated between $0\text{--}3 \text{ V}$ versus Li^+/Li and show a sloping charge–discharge profile,^[266] which is suitable for applications in capacitor-type devices. In 2012, Simon and Gogotsi et al. first attempted to fabricate a novel LIC using 2D Ti_2C as anode.^[58] When it was coupled with AC cathode, the LIC could store energy density of 15 Wh kg^{-1} at 0.6 kW kg^{-1} after 1000 cycles. Subsequently, Gogotsi et al. further prepared Nb_2CT_x -CNT films (delaminated Nb_2CT_x MXene with 10 wt% carbon nanotubes).^[267] Then, three kinds of LICs based on Nb_2CT_x -CNT: lithiated graphite// Nb_2CT_x -CNT, Nb_2CT_x -CNT// LiFePO_4 and lithiated Nb_2CT_x -CNT// Nb_2CT_x -CNT LICs were fabricated (as shown in Figure 21). The three LICs could provide energy densities of $50\text{--}70 \text{ Wh L}^{-1}$ within 3 V voltage windows. Due to typical 2D layer architecture of MXenes, they were easily aligned parallel to the current collector when producing electrode, which may limit the power density in some extent.

After that, inspired by the fascinating structure of the pillared interlayered clays (PILCs), Tao et al. fabricated pillared MXene ($\text{CTAB-Sn(IV)}@\text{Ti}_3\text{C}_2$) using a liquid-phase cetyltrimethylammonium bromide (CTAB) prepillaring and Sn⁴⁺ pillaring method,^[268] as shown in Figure 22a. Such method could enlarge the interlayer spacing of Ti_3C_2 , thus facilitating intercalation of Li^+ into Ti_3C_2 . Ultimately, the assembled $\text{CTAB-Sn(IV)}@\text{Ti}_3\text{C}_2$ //AC LIC showed an encouraging energy density of 45.31 Wh kg^{-1} at 10.8 kW kg^{-1} . Ma et al. recently developed a novel LIC consisting of binder-free flexible 2D titanium carbide/carbon nanotube composited ($\text{Ti}_3\text{C}_2\text{T}_x$ /CNT) film anode and AC cathode (Figure 22b).^[269] The addition of CNTs could effectively prevent $\text{Ti}_3\text{C}_2\text{T}_x$ from stacking. The $\text{Ti}_3\text{C}_2\text{T}_x$ /CNT (−)//AC (+) LIC showed an energy density of 67 Wh kg^{-1} at 258 W kg^{-1} .

10.3. 2D Sulfides (−)//Porous Carbon (+) LICs

Molybdenum disulfide (MoS_2), one of typically 2D sulfides has layered structure and been investigated as anode material for LIBs due to its high specific capacity (670 mAh g^{-1}) in a wide lithiation potential of $0.01\text{--}3 \text{ V}$ versus Li^+/Li .^[270] Nanostructured MoS_2 onto 3D graphene foam ($\text{MoS}_2@3\text{DG}$)^[59] and MoS_2 -ZIF composite (zeolitic imidazolate framework, ZIF-8, a subclass of MOFs)^[60] were the two recently developed materials used as anode of LICs. Typically, the $\text{MoS}_2@3\text{DG}/\text{NPC}$ (nitrogen-doped porous carbon) LIC could show 97 Wh kg^{-1} at 8.314 kW kg^{-1} and 78% of the initial capacity after 2000 cycles. The MoS_2 -ZIF//ZDPC (ZIF-8 derived porous carbon) LIC could maintain 44.7 Wh kg^{-1} at 20 kW kg^{-1} and show a rather low capacity fading of 0.0021% per cycle (10000 cycles). The conventional features of the above two composites were nanostructuring and hybridization with other conductive components to solve the unsatisfactory electric conductivity of MoS_2 .

10.4. Li_3VO_4 (−)//Porous Carbon (+) LICs

Sol-gel derived Li_3VO_4 was first used as an anode of LICs in combination with an AC cathode.^[271] However, the same to most of lithium ion intercalation materials, the poor electronic conductivity ($<10^{-10} \text{ S m}^{-1}$) of Li_3VO_4 material is detrimental to achieving high power performance. Naoi et al. designed an ultracentrifugation-derived nc- $\text{Li}_3\text{VO}_4/\text{MWCNT}$ composite. More than 50% capacity retention at 20 A g^{-1} (corresponding to a nearly 500 C rate, equal to 7.2 s) was retained. Afterward, N-doped carbon-encapsulated Li_3VO_4 nanowires ($\text{Li}_3\text{VO}_4\text{-NC NWs}$) were prepared by Yu et al., and presented an excellent rate pseudocapacitive behavior (271 mAh g^{-1} at 12 A g^{-1}).^[272] The $\text{Li}_3\text{VO}_4\text{-NC NWs}/\text{AC}$ LIC showed high operation voltage (4.0 V) and encouraging energy density (136.4 Wh kg^{-1}). Recently, Wu et al. designed a quasi-solid-state LIC consisting of Li_3VO_4 /carbon nanofibers anode and electrochemically reduced graphene sheets cathode.^[273] Due to the introduction of gel polymer electrolyte ($1 \text{ M LiClO}_4/\text{EC-DMC-DEC}$ in P(VDF-HFP)), the LIC did not catch fire and shrank when put in a flame. The safety issue was well guaranteed.

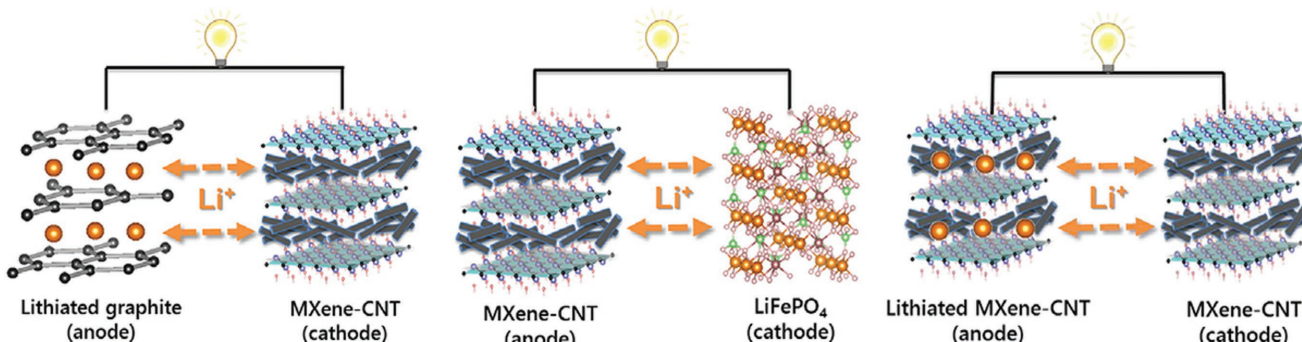


Figure 21. Three kinds of LICs with Nb_2CT_x -CNT as one electrode. Reproduced with permission.^[267] Copyright 2016, Elsevier.

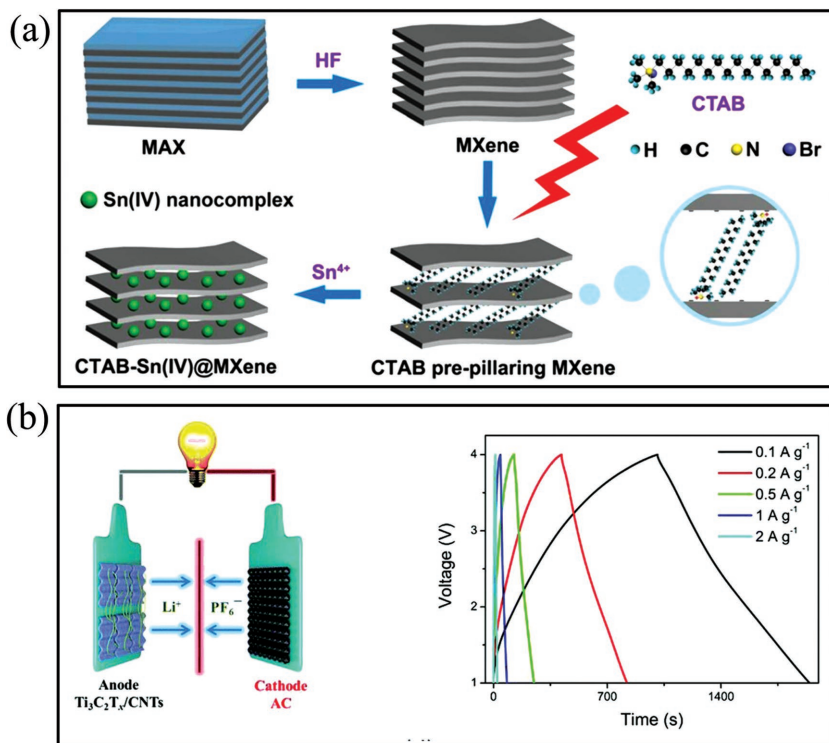


Figure 22. a) Schematic diagrams of synthesis of CTAB-Sn(IV)@ Ti₃C₂ by HF etching, CTAB prepillaring, and Sn⁴⁺ pillarating methods. Reproduced with permission.^[268] Copyright 2017, American Chemical Society. b) Schematic illustration of the Ti₃C₂T_x/CNT (–)//AC (+) LIC and the charge–discharge curves under various current density. Reproduced with permission.^[269] Copyright 2018, Royal Society of Chemistry.

11. Prelithiation Strategies

Take graphite//AC LIC system for example, the specific capacity of lithium ion intercalation graphite anode (300–350 mAh g⁻¹) is much higher than that of PF₆⁻ adsorbed AC cathode (30–50 mAh g⁻¹ in Li⁺ organic electrolyte). So, in order to get a capacity balance between AC cathode and graphite anode, the mass loading of AC on aluminum current collectors should be >5 times as much as that of graphite anode. However, the thick AC slurry coating on aluminum current collectors is rather challenging. Moreover, such thick electrode is easily peeled off from current collectors and can severely decrease the rate capability and cycleability.

Prelithiation toward anode is an effective way to inhibit these disadvantages.^[274,275] During the fabrication of LICs, metallic lithium or other lithium resources are placed at one side of the devices and served as the third electrode. Before charging the LIC, the metallic lithium electrode is connected with the graphite anode by short-circuiting directly, short circuiting through a resistor or galvanostatic discharging according to scheduled procedures on charge/discharge devices. Then metallic lithium is oxidized to be lithium ion into electrolyte. The lithium ions next to the anode are intercalated into graphite. Consequently, the potential of graphite anode decreases to near 0 V versus Li⁺/Li. Consequently, a flat and low potential anode is obtained, which enables a reduced electrode resistance and enhancement in energy density by allowing higher utilization of the

cathode within an enlarged voltage range (≥ 3.8 V). Furthermore, prelithiation process can also compensate for the poor efficiency during initial charge/discharge, alleviate the irreversible capacity and excessive consumption of electrolyte ions, which influence the stability of the anode and in turn the cell cycleability.^[82,276–278] According to the different lithium sources, it can be classified as metallic lithium metal oxide, and lithium ion from electrolyte.

11.1. Metallic Lithium

Initially, the lithium predoping strategy was designed for laminated electrodes and patented by Fuji Heavy Industry, Japan.^[279] Afterward, the strategy was also applied in cylindrical electrode by TAIYO YUDEN Co., Ltd.^[280] Prelithiation has also been intensively studied by many researchers as one of the most important technologies in LICs. As a conventional lithium resource, metallic lithium has been selected. Sivakumar et al. investigated the prelithiation of a graphite anode using three different techniques: i) short-circuiting the lithium with graphite anode externally, ii) short-circuiting with the aid of a suitable resistor, or iii) galvanostatic charging at C/20. The lithium predoping was terminated as soon

as the potential of Li/graphite reached to 0.05 V versus Li⁺/Li.^[82] Herein, the mass ratio of AC to graphite was equal. The way of prelithiation greatly affected the quality of the formed SEI layer, which in turn influenced the self-discharge characteristics of LICs. For directly short circuiting method, it might not form a uniform SEI. Consequently, the exposed parts of graphite anode would be in direct contact with the electrolyte, resulting in self-discharge. While the graphite anode being electrochemically doped at a rate of C/20 could produce a better SEI layer. However, similar self-discharge behaviors of the above two prelithiated anodes were all detected (Figure 23a,b). As far as the third prelithiation technique was concerned, it was carried out through short-circuiting the anode with lithium via a resistor and therefore, the anode potential reached to 0.05 V versus Li⁺/Li after ≈ 11 d. Encouragingly, this graphite anode showed a much slower self-discharge rate than that of the above two methods, (Figure 23c), which may be attributed to a satisfactory SEI film. Furthermore, a prolonged cycle performance of the cell for this technique was obtained. Therefore, the prelithiation technology and the forming SEI layer had a great influence on the quality of the prelithiated graphite anode, which in turn influenced the cycleability and self-discharge.

Koo et al. demonstrated a fast and efficient prelithiation method by internal short (IS), i.e., directly connecting the graphite electrode with lithium metal.^[80] Figure 24a showed the schematic diagrams of the IS method, electrochemical

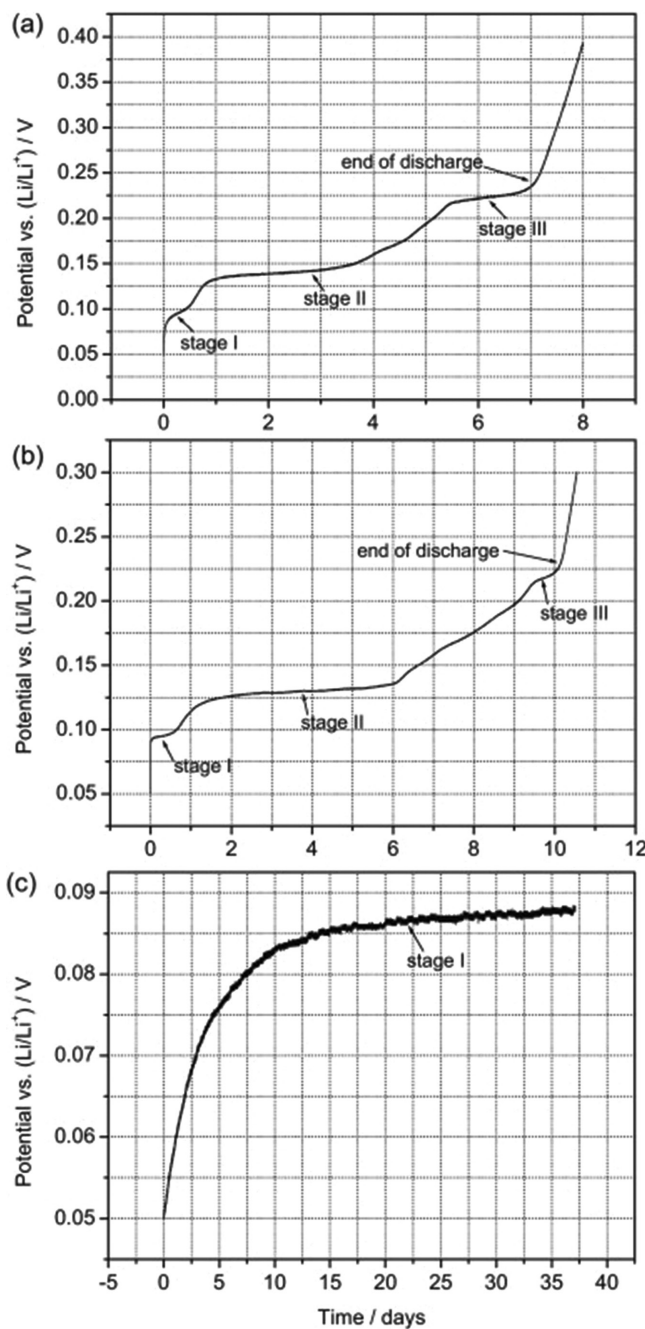


Figure 23. Self-discharge behavior of the prelithiated graphite anode, where the prelithiation techniques contained: a) directly short-circuiting for 10 h, b) discharging at C/20 rate, and c) short-circuiting with the aid of a resistor for 11 d. Reproduced with permission.^[82] Copyright 2012, Elsevier.

method (EC) and external short circuit (ESC) method. The EC prelithiation was conducted using an electronic charger with an option of constant cutoff voltage (0.05 V vs Li⁺/Li). The ESC prelithiation was performed by separating the graphite and lithium with a porous polyolefin separato, and externally connecting both of them using an electric cable. They concluded that EC and ESC techniques were rather time-consuming (>10 h), while the IS method could increase the prelithiation

rate to four times higher than that of the ES and ESC method. The potential difference and the distance between the graphite and the lithium significantly influenced the predoping rate. They also claimed that the IS method was free of safety issues, because the resistive graphite layer ($\approx 30 \Omega$ in the dry state) could function as a buffer layer and keep the potential difference between the graphite and lithium. Zheng et al. also reported a similar method with AC cathode and HC-SLMP anode electrodes.^[81] As shown in Figure 24b, the so-called SLMP was applied onto HC anode in order to avoid the consumption of the salt in electrolyte during cycling and achieved much higher specific energy and longer cycle life. No matter what prelithiation method being used, high efficiency and high quality electrode/electrolyte interface are the premise of the safety and cycleability of LICs. Followed by this work, they developed two LIC pouch cells LIC250 and LIC395 based on HC-SLMP (-)//AC (+) system.^[281] The SLMP was coated onto the HC anode using doctor blade method and then roll-pressed in a dry room, as illustrated in Figure 24c. The HC-SLMP (-)//AC (+) LIC showed a specific energy of 30 Wh kg⁻¹. The capacitance degradation was <20% even after 10000 cycles. However, the utilization of SLMP has some shortcomings. First, the safety issue should be concerned because the SLMP is hard to deal with and prone to scattered. Second, the purity of SLMP is only $\approx 98\%$, which results in high self-discharge rate and bad cycleability. Cao et al. reported a new-generation laminated LIC with thin lithium strips of 99.9% purity as the lithium sources applied on HC anode surface, which could maintain a DC life over 2000 h when held at 3.8 V under 65 °C.^[163]

A problem that cannot be ignored is the time-consuming of prelithiation. Generally, the prelithiation always takes dozens of hours or even tens of days, which brings huge time cost to commercial production. In order to optimize the time for prelithiation, Zheng et al. discussed five various prelithiation methods, as presented in Figure 25a–e.^[274] The results showed that Film20, Film15-25Li and Film15 could prelithiation in 2, 1, and < 1 h, respectively. However, the Strip45 spent 18 h for prelithiation. The holes on the lithium film could help the HC anode to make the soaking of electrolyte easy. Moreover, the thinner film could also improve the prelithiation. Finally, a 200 F LIC device was made to further illustrate the enhancement on power and energy output characteristics. Considering the fabrication complexity and cost, Film20 was identified as the best prelithiation method.

The prelithiation degree also deeply influences the electrochemical performance of LICs. It had been reported that in order to make the best of the AC cathode, prelithiation of the graphite anode should be controlled below $\approx 90\%$ because the specific capacity of the AC was determined to be $\approx 33 \text{ mAh g}^{-1}$.^[82] Shi et al. investigated the influence of prelithiation degrees on LICs. They found that the prelithiation degree had a great impact on energy density and cycleability.^[83] When the prelithiation was below 200 mAh g⁻¹, unsatisfactory cycle performance was presented (Figure 26). With the increased of prelithiation degree, the cycle performance was improved. When it was increased to 300 mAh g⁻¹, the LIC showed an energy density of 92.3 Wh kg⁻¹ and a power density of 5.5 kW kg⁻¹ and the best cycle life performance of $\approx 97.0\%$ retention after 1000 cycles, due to the maximized utilization of the AC cathode. However,

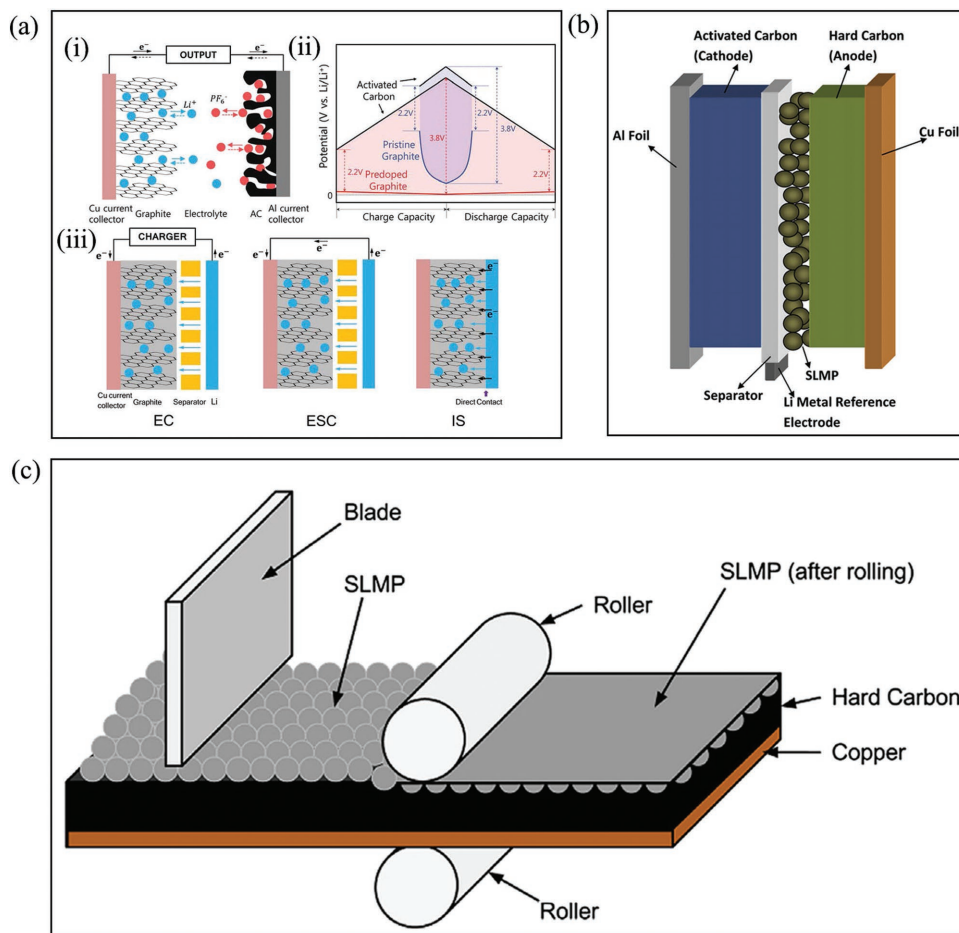


Figure 24. a) Prelithiation of graphite (–) // AC (+) LIC: i) schematic diagrams; ii) charge/discharge curves; iii) three kinds of prelithiation methods: EC, ESC, and IS. Reproduced with permission.^[80] Copyright 2014, Royal Society of Chemistry. b) Schematic diagram of an AC/HC-SLMP LIC. Reproduced with permission.^[81] Copyright 2012, Elsevier. c) Illustration of coating technique of SLMP on the anode. Reproduced with permission.^[282] Copyright 2017, Elsevier.

the cycle performance became bad when the prelithiation capacity reached to 350 mAh g⁻¹, due to the increase of resistance by the thick SEI film. Similar phenomena were also found by Yuan et al. and Sawa et al.^[282,283] Sawa et al. suggested that the prelithiation level could influence the specific capacitance, coulombic efficiency high and equivalent series resistance.^[267] The best electrochemical performance of LIC could be obtained when the prelithiation reached to was 71.1% (on the basis of the theoretical capacity of LiC₆). Although excessive prelithiation of 89.0% could deliver the highest specific capacitance, it resulted in bad cycle performance.

11.2. Lithium Metal Oxide

On the other hand, some researchers suggested that metallic lithium as the lithium source is somewhat unsafety because it can react with moisture under humid environment, causing safety issues, which would lead to potential safety issues. Moreover, it is very difficult to precisely load the proper amount of lithium ions.^[84] Excess metallic lithium would also cause safety

issues if improper prelithiation is implemented. In the past few years, many revolutionary and creative strategies have been proposed. Basically, electrochemical irreversible lithium metal oxides are chosen as lithium resources to substitute the metallic lithium. During the cell fabrication, the lithium metal oxide is quantitatively mixed with AC cathode. When the first discharge process begins (prelithiation), the Li⁺ is released from the cathode and intercalated into the anode. After that, Li⁺ is only partially recovered to the lithium metal oxides. By adjusting the amount of lithium metal oxides in the cathode, the prelithiation level is well controlled. Moreover, such electrochemical process is completed at high potential rather than metallic lithium at near 0 V versus Li⁺/Li, the decomposition of electrolyte oxidation can be effectively held back. Therefore, the overall process is controllable and safety. The electrochemical behaviors of Li₂MoO₃,^[84] Li₂RuO₃,^[284] Li₅FeO₄,^[285] Li₆CoO₄,^[286] Li_{0.65}Ni_{1.35}O₂,^[287] and Li₅ReO₆^[288] have been well investigated as lithium resource instead of metallic lithium. Take Li₂MoO₃ as lithium source for example. As shown in Figure 27, the conventional method is that the metallic lithium is placed at the anode side separated by separator or directly contacts with anode. By short-circuiting

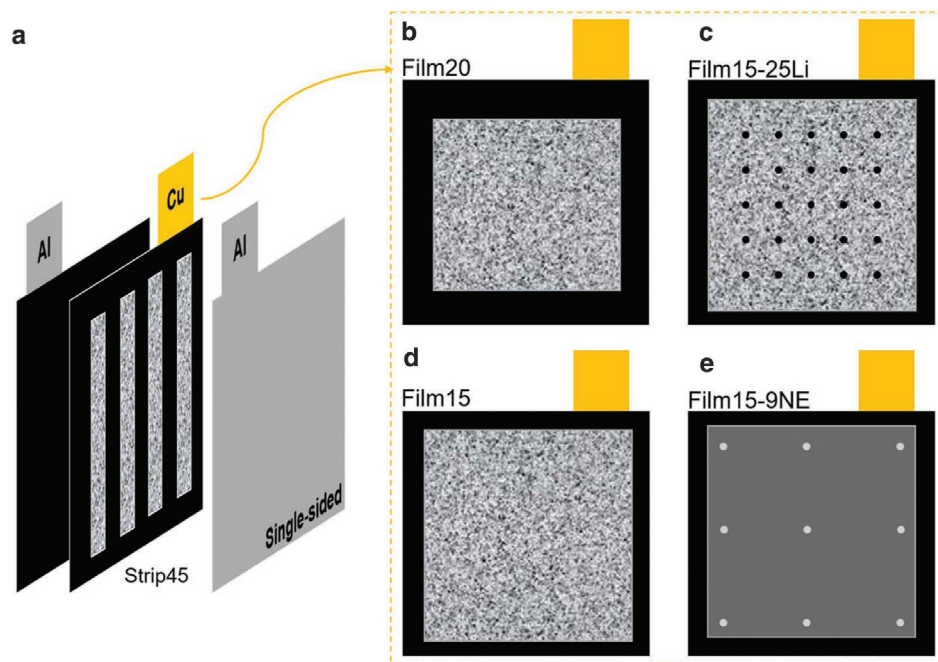


Figure 25. Schematics of sandwich LICs with five different prelithiation techniques on negative electrode. a) Sandwich cell with 45 μm Li strips, b) 20 μm Li thin film (size: 40 mm \times 40 mm), c) 15 μm Li thin film with 25 holes (size: 43 mm \times 43 mm), d) 15 μm Li thin film (size: 43 mm \times 43 mm), and e) 9 holes on negative electrode loaded with 15 μm Li thin film (size: 43 mm \times 43 mm). Reproduced with permission.^[274] Copyright 2017, The Electrochemical Society.

the metallic lithium and anode, lithium ions are inserted into anode. On the contrary, the proposed method is that Li_2MoO_3 is integrally mixed into the cathode. After the initial charging, lithium ions are intercalated into anode. As a result, the lithium-doping level and safety issues are well resolved.

11.3. Lithium Salt

Apart from metallic lithium or lithium metal oxides as lithium ion sources, electrolyte can also play an important role during

prelithiation. Very recently, Brousse et al. reported a “sacrificial organic lithium salt” prelithiation method, which used 3,4-dihydroxybenzonitrile dilithium salt (Li_2DHBN) as sacrificial salt in 1 M $\text{LiPF}_6/\text{EC-DMC}$, as presented in Figure 28.^[85] First, the cathode is formed by mixing the activated carbon, carbon black, insoluble Li_2DHBN and binder. Then, during the initial charge, the insoluble Li_2DHBN can irreversibly release Li^+ into electrolyte and obtain soluble 3,4-dioxobenzonitrile (DOBN), which in turn leads to the intercalation of Li^+ into graphite anode. In comparison with the conventional prelithiation method, the merit of this construction is free of the utilization of lithium metal, thus favoring a much safer and lower cost electrochemical device. When the AC (+)//graphite (-) LIC works at 2.2–4.0 V, the specific energies range from 40 to 60 Wh kg⁻¹ (per total mass of electrode materials) under various charge-discharge modes.

12. Conclusion and Perspective

Nonaqueous LICs, due to their high energy density, high power density and long cycle life, have been received more and more attention. Various materials, varied strategies, and diversified LIC systems have been well developed. The core issues of all LIC systems are: a) enhancing the electrochemical kinetic behaviors of lithium intercalation/deintercalation; b) designing suitable electrode materials to improve the energy density at high power density; c) choosing proper prelithiation methods to receive an extended voltage window, a high efficient cell production and a long cycle life. Tremendous efforts have been made, including:

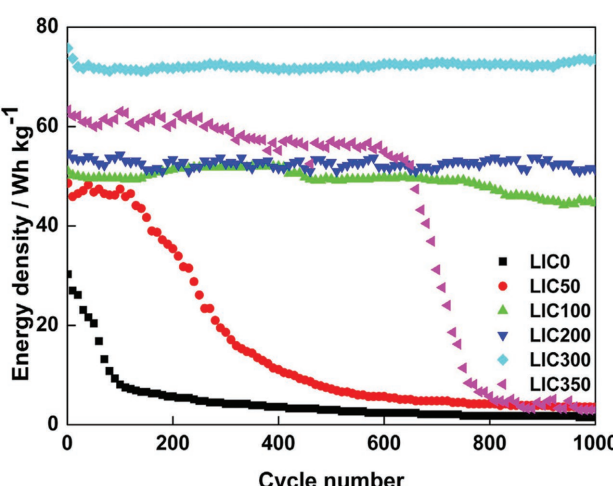


Figure 26. Cycle life of LICs using 1.2 M $\text{LiPF}_6/\text{EC-DEC}$ at 2 C rate. The numbers in the abbreviation stand for the prelithiation capacity. Reproduced with permission.^[83] Copyright 2014, Elsevier.

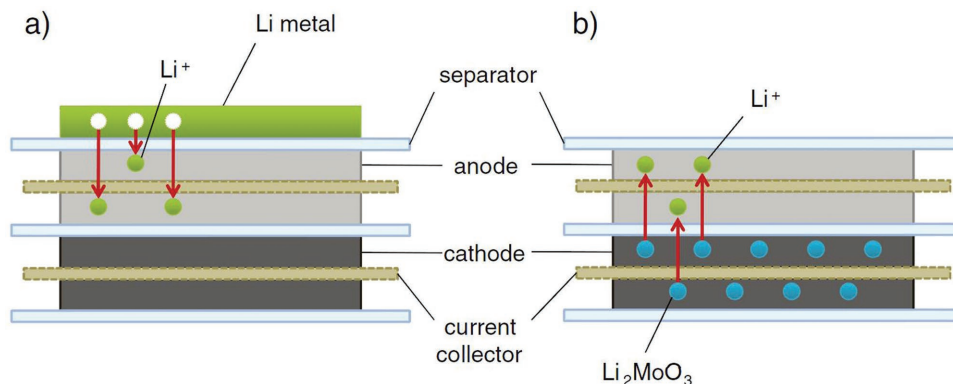


Figure 27. Schematic diagrams showing different prelithiation methods: a) conventional lithium doping using metallic lithium in the cell and b) proposed method using Li_2MoO_3 as an alternative lithium source. Reproduced with permission.^[283] Copyright 2011, Wiley-VCH.

Cathode Materials: For most of LIC system, cathode materials are generally based on porous carbon, typically activated carbon. The merits of active carbon is high specific surface area, porous structure and low prices, which is favorable to ion adsorption/diffusion and cost-effectiveness. However, the low specific capacity of activated carbon limits the energy density of LICs. The electrical conductivity of activated carbon should also be further improved. Multilevel ordering structure, element doping, rational pore structure design, combining with LIB cathode materials, and so on, are the main principles of improving the electrochemical performance of LIC cathode.

Anode Materials: Most of the LIC anode materials are based on electrochemical intercalation/deintercalation mechanisms, which lead to a mismatched electrochemical kinetics with physical adsorption/desorption cathode. Therefore, the rate capability, or power output of LICs is greatly restricted. A core assignment is to improve the dynamic performance, typically, ion diffusion/transportation in the bulk. Nanosizing/morphological control, elemental doping, formation of composites, etc., are the fundamental methods to enhance the ion diffusion/transportation and electron transfer behaviors. By reducing the particle size into nano scale, the transport distance of lithium ions can be drastically shortened, which results in fast lithium ion diffusion kinetics, high the electrode-electrolyte contact area and excellent rate capability. However, there are still some other disadvantages, such as tedious synthesis process, rigorous slurry mixing conditions, side reaction between the electrode

and decreased volumetric energy density of the device. The formation of composites is usually achieved by coating or mixing with conductive carbon. Both electronic and lithium ion conductivity could be highly improved. The cost advantage of this method is obvious. Nevertheless, such methods only change the surface chemistry property. Element doping can adjust the inner electronic structure of electrode materials, resulting in an increased electrical conductivity and a superior lithium ion intercalation/deintercalation property. Nevertheless, element doping usually involves the use of precious metals, and the preparation process is rather tedious. Therefore, the best way is to select appropriate modification methods according to the characteristics of the material system. With the rapid development of novel 2D materials, such as graphene, Mxenes, sulfides, etc., there will be more and more advanced energy materials with high ion and electron conductivity using advanced material preparation techniques.

Prelithiation: Prelithiation is an effective way to extend the electrochemical window, compensate for the initial loss during the formation of SEI, balance the anode and cathode, and obtain an excellent cycle performance of LICs. Various methods have been investigated. The type of lithium sources, the way of prelithiation, the amount of prelithiation, and the structure of anode materials play important roles on the electrochemical performances of LICs. These factors have substantial effects on SEI, electrode/electrolyte interface, resistance, self-discharge, cycleability, and eventually the energy density and power density.

From a commercial production point of view, it influences the production technology and cost. Therefore, it is very important to select suitable prelithiation method to ensure production efficiency, low production cost, and high safety.

Safety Issues: LIC is a kind of high power input/output energy storage devices, so the safety issues are of great importance. By selecting the optimized electrode materials and scientific cell structure design, which can greatly decrease the internal resistance, the power capability can be highly improved. Solid state electrolytes are currently the most popular technique to solve

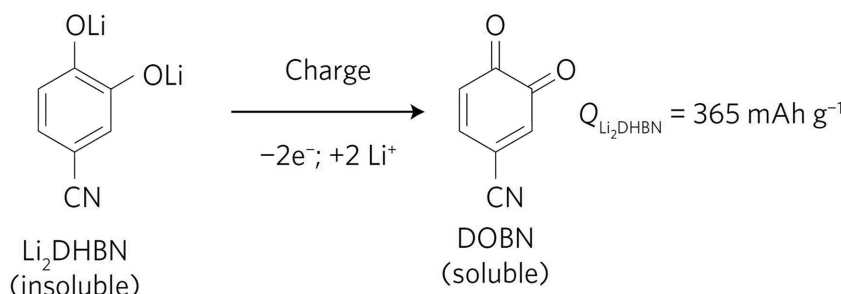


Figure 28. A schematic diagram of Li_2DHBNCN oxidized to DOBN. The reaction consists of the delithiation of an Li_2DHBNCN in order to obtain DOBN. Reproduced with permission.^[85] Copyright 2018, Nature Publishing Group.

the safety issues due to utilization of flammable organic liquid electrolytes.

Currently, the development of LICs is in an embarrassing situation because of the relatively low energy/cost ratio based on the present technology. Although basic research is very active, large scale commercial applications are not yet available in the market. If the energy density can be highly retained even at super high power density, the LICs will be widely accepted by high-end market, especially in the field of braking energy recovery, emergency starting/back-up power supply, stabilization of electric power quality, and so on.

Acknowledgements

This work was supported by the Youth Innovation Promotion Association CAS (Grant No. 2017253), the National Natural Science Foundation for Distinguished Young Scholars of China (Grant No. 51625204), the National Key R&D Program of China (Grant No. 2018YFB0104300), the Key Research Program of the Chinese Academy of Sciences (Grant No. KFZD-SW-414), the Key Scientific and Technological Innovation Project of Shandong (Grant No. 2017CXZC0505), and the Qingdao Key Lab of solar energy utilization and energy storage technology.

Conflict of Interest

The authors declare no conflict of interest.

Keywords

energy storage, lithium ion capacitor, material design, organic electrolyte, prelithiation

Received: April 25, 2018

Revised: July 23, 2018

Published online:

- [1] N. Kittner, F. Lill, D. M. Kammen, *Nat. Energy* **2017**, *2*, 17125.
- [2] W. A. Braff, J. M. Mueller, J. E. Trancik, *Nat. Clim. Change* **2016**, *6*, 964.
- [3] N.-S. Choi, Z. Chen, S. A. Freunberger, X. Ji, Y.-K. Sun, K. Amine, G. Yushin, L. F. Nazar, J. Cho, P. G. Bruce, *Angew. Chem., Int. Ed.* **2012**, *51*, 9994.
- [4] F. Wang, X. Wu, X. Yuan, Z. Liu, Y. Zhang, L. Fu, Y. Zhu, Q. Zhou, Y. Wu, W. Huang, *Chem. Soc. Rev.* **2017**, *46*, 6816.
- [5] D. D. Lecce, R. Verrelli, J. Hassoun, *Green Chem.* **2017**, *19*, 3442.
- [6] Y. Wang, Y. Song, Y. Xia, *Chem. Soc. Rev.* **2016**, *45*, 5925.
- [7] M. Inagaki, H. Konno, O. Tanaike, *J. Power Sources* **2010**, *195*, 7880.
- [8] L. Zhou, K. Zhang, Z. Hu, Z. Tao, L. Mai, Y.-M. Kang, S.-L. Chou, J. Chen, *Adv. Energy Mater.* **2017**, *7*, 1701415.
- [9] A. Manthiram, *ACS Cent. Sci.* **2017**, *3*, 1063.
- [10] S. Xin, Y. You, S. Wang, H.-C. Gao, Y.-X. Yin, Y.-G. Guo, *ACS Energy Lett.* **2017**, *2*, 1385.
- [11] Y. Zhai, Y. Dou, D. Zhao, P. F. Fulvio, R. T. Mayes, S. Dai, *Adv. Mater.* **2011**, *23*, 4828.
- [12] R. R. Salunkhe, Y.-H. Lee, K.-H. Chang, J.-M. Li, P. Simon, J. Tang, N. L. Torad, C.-C. Hu, Y. Yamauchi, *Chem. – Eur. J.* **2014**, *20*, 13838.
- [13] D. Cericola, R. Kötz, *Electrochim. Acta* **2012**, *72*, 1.

- [14] H. Wang, C. Zhu, D. Chao, Q. Yan, H. J. Fan, *Adv. Mater.* **2017**, *29*, 1702093.
- [15] B. Li, J. Zheng, H. Zhang, L. Jin, D. Yang, H. Lv, C. Shen, A. Shellikeri, Y. Zheng, R. Gong, J. P. Zheng, C. Zhang, *Adv. Mater.* **2018**, *30*, 1705670.
- [16] J. Lang, X. Zhang, B. Liu, R. Wang, J. Chen, X. Yan, *J. Energy Chem.* **2018**, *27*, 43.
- [17] A. Cappetto, W. J. Cao, J. F. Luo, M. Hagen, D. Adams, A. Shellikeri, K. Xue, J. P. Zheng, *J. Power Sources* **2017**, *359*, 205.
- [18] S. Barcellona, L. Piegarì, *J. Power Sources* **2017**, *342*, 241.
- [19] G. Wang, C. Lu, X. Zhang, B. Wan, H. Liu, M. Xia, H. Gou, G. Xin, J. Lian, Y. Zhang, *Nano Energy* **2017**, *36*, 46.
- [20] X. Zhang, C. Lu, H. Peng, X. Wang, Y. Zhang, Z. Wang, Y. Zhong, G. Wang, *Electrochim. Acta* **2017**, *246*, 1237.
- [21] A. Jaina, S. Jayaraman, M. Ulaganathan, R. Balasubramanian, V. Aravindan, M. P. Srinivasane, S. Madhavi, *Electrochim. Acta* **2017**, *228*, 131.
- [22] B. Li, H. Zhang, D. Wang, H. Lv, C. Zhang, *RSC Adv.* **2017**, *7*, 37923.
- [23] Z. Yang, H. Guo, X. Li, Z. Wang, J. Wang, Y. Wang, Z. Yan, D. Zhang, *J. Mater. Chem. A* **2017**, *5*, 15302.
- [24] M. Halim, G. Liu, R. E. A. Ardhi, C. Hudaya, O. Wijaya, S.-H. Lee, A.-Y. Kim, J. K. Lee, *ACS Appl. Mater. Interfaces* **2017**, *9*, 20566.
- [25] B. Li, Z. Xiao, M. Chen, Z. Huang, X. Tie, J. Zai, X. Qian, *J. Mater. Chem. A* **2017**, *5*, 24502.
- [26] M. Saito, K. Takahashi, K. Ueno, S. Seki, *J. Electrochem. Soc.* **2016**, *163*, A3140.
- [27] P. Sennu, V. Aravindan, Y.-S. Lee, *Chem. Eng. J.* **2017**, *324*, 26.
- [28] J. Ajuria, M. Arnaiz, C. Botas, D. Carriazo, R. Mysyk, T. Rojo, A. V. Talyzin, E. Goikolea, *J. Power Sources* **2017**, *363*, 422.
- [29] G. Tang, L. Cao, P. Xiao, Y. Zhang, H. Liu, *J. Power Sources* **2017**, *355*, 1.
- [30] D. Ruan, Y. Huang, L. Li, J. Yuan, Z. Qiao, *J. Alloys Compd.* **2017**, *695*, 1685.
- [31] J. Boltersdorf, S. A. Delp, J. Yan, B. Cao, J. P. Zheng, T. R. Jow, J. A. Read, *J. Power Sources* **2018**, *373*, 20.
- [32] N. Xu, X. Sun, F. Zhao, X. Jin, X. Zhang, K. Wang, K. Huang, Y. Ma, *Electrochim. Acta* **2017**, *236*, 443.
- [33] Q. Xia, H. Yang, M. Wang, M. Yang, Q. Guo, L. Wan, H. Xia, Y. Yu, *Adv. Energy Mater.* **2017**, *7*, 1701336.
- [34] X. Xu, Y. Cui, J. Shi, W. Liu, *RSC Adv.* **2017**, *7*, 17178.
- [35] Y. Sun, J. Tang, F. Qin, J. Yuan, K. Zhang, J. Li, D.-M. Zhu, L.-C. Qin, *J. Mater. Chem. A* **2017**, *5*, 13601.
- [36] J.-A. Wang, S.-M. Li, Y.-S. Wang, P.-Y. Lan, W.-H. Liao, S.-T. Hsiao, S.-C. Lin, C.-W. Lin, C.-C. M. Ma, C.-C. Hu, *J. Electrochem. Soc.* **2017**, *164*, A3657.
- [37] S. Yata, Y. Hato, K. Sakurai, T. Osaki, K. Tanaka, T. Yamabe, *Synth. Met.* **1987**, *18*, 645.
- [38] S. Yata, E. Okamoto, H. Satake, H. Kubota, M. Fujii, T. Taguchi, H. Kinoshita, *J. Power Sources* **1996**, *60*, 207.
- [39] S. Yata, Y. Hato, H. Kinoshita, N. Ando, A. Anekawa, T. Hashimoto, M. Yamaguchi, K. Tanaka, T. Yamabe, *Synth. Met.* **1995**, *73*, 273.
- [40] T. Morimoto, M. Tsushima, Y. Che, presented at *Symposium on New Materials for Batteries and Fuel Cells*, Materials Research Society, San Francisco, USA **1999**, p. 4.
- [41] T. Morimoto, *Electrochemistry* **2000**, *68*, 1012.
- [42] G. G. Amatucci, F. Badway, A. DuPasquier, *ECS Proc.* **2000**, *99*, 344.
- [43] A. D. Pasquier, I. Plitz, J. Gural, F. Badway, G. G. Amatucci, *J. Power Sources* **2004**, *136*, 160.
- [44] K. Naoi, W. Naoi, S. Aoyagi, J. Miyamoto, T. Kamino, *Acc. Chem. Res.* **2013**, *21*, 1075.
- [45] K. Naoi, *Fuel Cells* **2010**, *10*, 825.

- [46] S. Ando, S. Tazaki, T. Fujii, K. Kojima, K. Matui, O. Hatozaki, Y. Hato, H. Shibuya, presented at *The 46th Battery Symposium in Japan*, Nagoya, Japan **2005**, p. 10.
- [47] K. Naoi, S. Ishimoto, J.-I. Miyamoto, W. Naoi, *Energy Environ. Sci.* **2012**, 5, 9363.
- [48] H. Li, L. Cheng, Y. Xia, *Electrochim. Solid-State Lett.* **2005**, 8, A433.
- [49] T. Brousse, R. Marchand, P.-L. Taberna, P. Simon, *J. Power Sources* **2006**, 158, 571.
- [50] Q. Wang, Z. Wen, J. Li, *Adv. Funct. Mater.* **2006**, 16, 2141.
- [51] H. Konno, T. Kasashima, K. Azumi, *J. Power Sources* **2009**, 191, 623.
- [52] B. Z. Jang, C. Liu, D. Neff, Z. Yu, M. C. Wang, W. Xiong, A. Zhamu, *Nano Lett.* **2011**, 11, 3785.
- [53] S. Dong, X. Chen, L. Gu, X. Zhou, H. Xu, H. Wang, Z. Liu, P. Han, J. Yao, L. Wang, G. Cui, L. Chen, *ACS Appl. Mater. Interfaces* **2011**, 3, 93.
- [54] P. Han, Y. Yue, X. Wang, W. Ma, S. Dong, K. Zhang, C. Zhang, G. Cui, *J. Mater. Chem.* **2012**, 22, 24918.
- [55] P. Han, W. Ma, S. Pang, Q. Kong, J. Yao, C. Bi, G. Cui, *J. Mater. Chem. A* **2013**, 1, 5949.
- [56] W. Ma, P. Han, Q. Kong, K. Zhang, C. Bi, G. Cui, *J. Inorg. Mater.* **2013**, 28, 733.
- [57] M. Liu, L. Zhang, P. Han, X. Han, H. Du, X. Yue, Z. Zhang, H. Zhang, G. Cui, *Part. Part. Syst. Charact.* **2015**, 32, 1006.
- [58] J. Come, M. Naguib, P. Rozier, M. W. Barsoum, Y. Gogotsi, P.-L. Taberna, M. Morcrette, P. Simon, *J. Electrochem. Soc.* **2012**, 159, A1368.
- [59] F. Zhang, Y. Tang, H. Liu, H. Ji, C. Jiang, J. Zhang, X. Zhang, C.-S. Lee, *ACS Appl. Mater. Interfaces* **2016**, 8, 4691.
- [60] R. Wang, D. Jin, Y. Zhang, S. Wang, J. Lang, X. Yan, L. Zhang, *J. Mater. Chem. A* **2017**, 5, 292.
- [61] W. Qi, J. G. Shapter, Q. Wu, T. Yin, G. Gao, D. Cui, *J. Mater. Chem. A* **2017**, 5, 19521.
- [62] G. Zhang, X. Xiao, B. Li, P. Gu, H. Xue, H. Pang, *J. Mater. Chem. A* **2017**, 5, 8155.
- [63] S. W. Bokhari, A. H. Siddique, H. Pan, Y. Li, M. Imtiaz, Z. Chen, S. M. Zhu, D. Zhang, *RSC Adv.* **2017**, 7, 18926.
- [64] T. Kou, B. Yao, T. Liu, Y. Li, *J. Mater. Chem. A* **2017**, 5, 17151.
- [65] S. Li, J. Chen, M. Cui, G. Cai, J. Wang, P. Cui, X. Gong, P. S. Lee, *Small* **2017**, 13, 1602893.
- [66] D.-Y. Sin, B.-R. Koo, H.-J. Ahn, *J. Alloys Compd.* **2017**, 696, 290.
- [67] S. Zhang, C. Li, X. Zhang, X. Sun, K. Wang, Y. Ma, *ACS Appl. Mater. Interfaces* **2017**, 9, 17136.
- [68] A. Eftekhari, Z. Fan, *Mater. Chem. Front.* **2017**, 1, 1001.
- [69] H. Liu, X. Liu, W. Li, X. Guo, Y. Wang, G. Wang, D. Zhao, *Adv. Energy Mater.* **2017**, 7, 1700283.
- [70] Y.-Y. Zhu, Y. Guo, C.-Y. Wang, Z.-J. Qiao, M.-M. Chen, *Chem. Eng. Sci.* **2015**, 135, 109.
- [71] B. Wang, C. Hu, L. Dai, *Chem. Commun.* **2016**, 52, 14350.
- [72] Q. Wei, F. Xiong, S. Tan, L. Huang, E. H. Lan, B. Dunn, L. Mai, *Adv. Mater.* **2017**, 29, 1602300.
- [73] P. Solís-Fernández, M. Bissett, H. Ago, *Chem. Soc. Rev.* **2017**, 46, 4572.
- [74] T. Liu, F. Zhang, Y. Song, Y. Li, *J. Mater. Chem. A* **2017**, 5, 17705.
- [75] Q. Shi, Y. Cha, Y. Song, J.-I. Lee, C. Zhu, X. Li, M.-K. Song, D. Du, Y. Lin, *Nanoscale* **2016**, 8, 15414.
- [76] Hao Lu, X. S. Zhao, *Sustainable Energy Fuels* **2017**, 1, 1265.
- [77] L. Wang, D. Chen, K. Jiang, G. Shen, *Chem. Soc. Rev.* **2017**, 46, 6764.
- [78] J. Deng, M. Li, Y. Wang, *Green Chem.* **2016**, 18, 4824.
- [79] N. Chaoui, M. Trunk, R. Dawson, J. Schmidt, A. Thomas, *Chem. Soc. Rev.* **2017**, 46, 3302.
- [80] M. Kim, F. Xu, J. H. Lee, C. Jung, S. M. Hong, Q. M. Zhang, C. M. Koo, *J. Mater. Chem. A* **2014**, 2, 10029.
- [81] W. J. Cao, J. P. Zheng, *J. Power Sources* **2012**, 213, 180.
- [82] S. R. Sivakkumar, A. G. Pandolfo, *Electrochim. Acta* **2012**, 65, 280.
- [83] J. Zhang, Z. Shi, C. Wang, *Electrochim. Acta* **2014**, 125, 22.
- [84] M.-S. Park, Y.-G. Lim, J.-H. Kim, Y.-J. Kim, J. Cho, J.-S. Kim, *Adv. Energy Mater.* **2011**, 1, 1002.
- [85] P. Jeżowski, O. Crosnier, E. Deunf, P. Poizot, F. Béguin, T. Brousse, *Nat. Mater.* **2018**, 17, 167.
- [86] C. Han, Y.-B. He, M. Liu, B. Li, Q.-H. Yang, C.-P. Wong, F. Kang, *J. Mater. Chem. A* **2017**, 5, 6368.
- [87] G. Xu, P. Han, S. Dong, H. Liu, G. Cui, L. Chen, *Coord. Chem. Rev.* **2017**, 343, 139.
- [88] G. G. Amatucci, F. Badway, A. D. Pasquier, T. Zheng, *J. Electrochem. Soc.* **2001**, 148, A930.
- [89] A. D. Pasquier, I. Plitz, J. Gural, S. Menocal, G. Amatucci, *J. Power Sources* **2003**, 113, 62.
- [90] L. Cheng, H.-J. Liu, J.-J. Zhang, H.-M. Xiong, Y.-Y. Xia, *J. Electrochem. Soc.* **2006**, 153, A1472.
- [91] S. Deng, J. W. Li, S. B. Sun, H. Wang, J. B. Liu, H. Yan, *Electrochim. Acta* **2014**, 146, 37.
- [92] B.-G. Lee, S.-H. Lee, *J. Power Sources* **2017**, 343, 545.
- [93] H.-G. Jung, N. Venugopal, B. Scrosati, Y.-K. Sun, *J. Power Sources* **2013**, 221, 266.
- [94] B. Zhao, R. Ran, M. Liu, Z. Shao, *Mater. Sci. Eng., R* **2015**, 98, 1.
- [95] L. Cheng, X.-L. Li, H.-J. Liu, H.-M. Xiong, P.-W. Zhang, Y.-Y. Xia, *J. Electrochem. Soc.* **2007**, 154, A692.
- [96] J. Ni, L. Yang, H. Wang, L. Gao, *J. Solid State Electrochem.* **2012**, 16, 2791.
- [97] A. Vijayakumar, R. Rajagopalan, A. S. Susharnakumariamma, J. Joseph, A. Ajaya, S. V. Nair, M. S. D. Krishna, A. Balakrishnan, *J. Energy Chem.* **2015**, 24, 337.
- [98] L. Ye, Q. Liang, Y. Lei, X. Yu, C. Han, W. Shen, Z.-H. Huang, F. Kang, Q.-H. Yang, *J. Power Sources* **2015**, 282, 174.
- [99] B. Lee, J. R. Yoon, *Curr. Appl. Phys.* **2013**, 13, 1350.
- [100] S. Dong, X. Wang, L. Shen, H. Li, J. Wang, P. Nie, J. Wang, X. Zhang, *J. Electroanal. Chem.* **2015**, 757, 1.
- [101] H. S. Choi, T. H. Kim, J. H. Im, C. R. Park, *Nanotechnology* **2011**, 22, 405402.
- [102] H. S. Choi, J. H. Im, T. Kim, J. H. Park, C. R. Park, *J. Mater. Chem.* **2012**, 22, 16986.
- [103] H. Xu, X. Hun, Y. Sun, W. Luo, C. Chen, Y. Liu, Y. Huang, *Nano Energy* **2014**, 10, 163.
- [104] Z. Lei, J. Zhang, L. L. Zhang, N. A. Kumard, X. S. Zhao, *Energy Environ. Sci.* **2016**, 9, 1891.
- [105] J.-Y. Liu, X.-X. Li, J.-R. Huang, J.-J. Li, P. Zhou, J.-H. Liu, X.-J. Huang, *J. Mater. Chem. A* **2017**, 5, 5977.
- [106] H. Kim, K.-Y. Park, M.-Y. Cho, M.-H. Kim, J. Hong, S.-K. Jung, K. Ch. Roh, K. Kang, *ChemElectroChem* **2014**, 1, 125.
- [107] T. Yuan, W.-T. Li, W. Zhang, Y.-S. He, C. Zhang, X.-Z. Liao, Z.-F. Ma, *Ind. Eng. Chem. Res.* **2014**, 53, 10849.
- [108] R. Xue, J. Yan, L. Jiang, B. Yi, *Mater. Chem. Phys.* **2015**, 160, 375.
- [109] N. Xu, X. Sun, X. Zhang, K. Wang, Y. Ma, *RSC Adv.* **2015**, 5, 94361.
- [110] C. Fu, L. J. Zhang, J. H. Peng, H. Wang, H. Yan, *Ionics* **2016**, 22, 1829.
- [111] C. Lua, X. Wang, X. Zhang, H. Peng, Y. Zhang, G. Wang, Z. Wang, G. Cao, N. Umriov, Z. Bakenov, *Ceram. Int.* **2017**, 43, 6554.
- [112] Q. Wang, J. Yan, Z. Fan, *Energy Environ. Sci.* **2016**, 9, 729.
- [113] X. Yao, Y. L. Zhao, *Chemistry* **2017**, 2, 171.
- [114] T. N. Phan, M. K. Gong, R. Thangavel, Y. S. Lee, C. H. Ko, *J. Alloys Compd.* **2018**, 743, 639.
- [115] Y. Lei, Z.-H. Huang, Y. Yang, W. Shen, Y. Zheng, H. Sun, F. Kang, *Sci. Rep.* **2013**, 3, 2477.
- [116] M. D. Stoller, S. Murali, N. Quarles, Y. Zhu, J. R. Potts, X. Zhu, H.-W. Ha, R. S. Ruoff, *Phys. Chem. Chem. Phys.* **2012**, 14, 3388.
- [117] V. Aravindan, D. Mhamane, W. C. Ling, S. Ogale, S. Madhavi, *ChemSusChem* **2013**, 6, 2240.

- [118] Q. Fan, M. Yang, Q. Meng, B. Cao, Y. Yu, *J. Electrochem. Soc.* **2016**, 163, A1736.
- [119] J. H. Won, H. M. Jeong, J. K. Kang, *Adv. Energy Mater.* **2017**, 7, 1601355.
- [120] J. Wang, P. Nie, B. Ding, S. Dong, X. Hao, H. Dou, X. Zhang, *J. Mater. Chem. A* **2017**, 5, 2411.
- [121] W. Long, B. Fang, A. Ignaszak, Z. Wu, Y.-J. Wang, D. Wilkinson, *Chem. Soc. Rev.* **2017**, 46, 7176.
- [122] Y.-P. Gao, Z.-B. Zhai, K.-J. Huang, Y.-Y. Zhang, *New J. Chem.* **2017**, 41, 11456.
- [123] R. Thangavel, K. Kaliyappan, H. V. Ramasamy, X. Sun, Y.-S. Lee, *ChemSusChem* **2017**, 10, 2805.
- [124] A. Jain, V. Aravindan, S. Jayaraman, P. S. Kumar, R. Balasubramanian, S. Ramakrishna, S. Madhavi, M. P. Srinivasan, *Sci. Rep.* **2013**, 3, 3002.
- [125] P. Sennu, H.-J. Choi, S.-G. Baek, V. Aravindan, Y.-S. Lee, *Carbon* **2016**, 98, 58.
- [126] R. Satish, V. Aravindan, W. C. Ling, N. K. Woei, S. Madhavi, *Electrochim. Acta* **2015**, 182, 474.
- [127] B. Babu, P. G. Lashmi, M. M. Shajumon, *Electrochim. Acta* **2016**, 211, 289.
- [128] J. Jiang, P. Nie, B. Ding, Y. Zhang, G. Xu, L. Wu, H. Dou, X. Zhang, *J. Mater. Chem. A* **2017**, 5, 23283.
- [129] R. Gokhale, V. Aravindan, P. Yadav, S. Jain, D. Phase, S. Madhavi, S. Ogale, *Carbon* **2014**, 80, 462.
- [130] D. Puthusseri, V. Aravindan, S. Madhavi, S. Ogalea, *Electrochim. Acta* **2014**, 130, 766.
- [131] A. Banerjee, K. K. Upadhyay, D. Puthusseri, V. Aravindan, S. Madhavi, S. Ogale, *Nanoscale* **2014**, 6, 4387.
- [132] D. Mhamane, V. Aravindan, M.-S. Kim, H.-K. Kim, K. C. Roh, D. Ruan, S. H. Lee, M. Srinivasan, K.-B. Kim, *J. Mater. Chem. A* **2016**, 4, 5578.
- [133] S. Park, Y. G. Yoo, I. Nam, S. Bae, J. Park, J. W. Han, J. Yi, *ACS Appl. Mater. Interfaces* **2016**, 8, 12186.
- [134] Q. Guo, L. Chen, Z. Shan, W. S. V. Lee, W. Xiao, Z. Liu, J. Liang, G. Yang, J. Xue, *ChemSusChem* **2017**, 10, 1.
- [135] J. H. Lee, H.-K. Kim, S.-H. Lee, *J. Alloys Compd.* **2017**, 695, 787.
- [136] J. H. Lee, H.-K. Kim, S.-H. Lee, *J. Power Sources* **2017**, 343, 545.
- [137] G.-N. Zhu, Y.-G. Wang, Y.-Y. Xia, *Energy Environ. Sci.* **2012**, 5, 6652.
- [138] S.-H. Lee, H.-K. Kim, J. H. Lee, S.-G. Lee, Y.-H. Lee, *Mater. Lett.* **2015**, 143, 101.
- [139] S.-H. Lee, S.-G. Lee, J.-R. Yoon, H.-K. Kim, *J. Power Sources* **2015**, 273, 839.
- [140] J.-R. Yoon, E. Baek, H.-K. Kim, M. Pecht, S.-H. Lee, *Carbon* **2016**, 101, 9.
- [141] J.-H. Kim, S.-H. Lee, *J. Power Sources* **2016**, 331, 1.
- [142] J. H. Lee, H.-K. Kim, E. Baek, M. Pecht, S.-H. Lee, Y.-H. Lee, *J. Power Sources* **2016**, 301, 348.
- [143] J. H. Kim, J.-R. Yoon, S.-H. Lee, *Electrochim. Acta* **2016**, 220, 231.
- [144] S. Flandrois, B. Simon, *Carbon* **1999**, 37, 195.
- [145] V. Khomenko, E. Raymundo-Piñero, F. Béguin, *J. Power Sources* **2008**, 177, 643.
- [146] S. R. Sivakkumar, J. Y. Nerkar, A. G. Pandolfo, *Electrochim. Acta* **2010**, 55, 3330.
- [147] S. R. Sivakkumar, A. S. Milev, A. G. Pandolfo, *Electrochim. Acta* **2011**, 56, 9700.
- [148] Y.-G. Lim, J. W. Park, M.-S. Park, D. Byun, J.-S. Yu, Y. N. Jo, Y.-J. Kim, *Bull. Korean Chem. Soc.* **2015**, 36, 150.
- [149] J. H. Lee, W. H. Shin, S. Y. Lim, B. G. Kim, J. W. Choi, *Mater. Renewable Sustainable Energy* **2014**, 3, 22.
- [150] X. Han, P. Han, J. Yao, S. Zhang, X. Cao, J. Xiong, J. Zhang, G. Cui, *Electrochim. Acta* **2016**, 196, 603.
- [151] F. Sun, J. Gao, X. Liu, L. Wang, Y. Yang, X. Pi, S. Wu, Y. Qin, *Electrochim. Acta* **2016**, 213, 626.
- [152] S.-O. Kim, H. S. Kim, J. K. Lee, *Mater. Chem. Phys.* **2012**, 133, 38.
- [153] Z. Yang, H. Guo, X. Li, Z. Wang, Z. Yan, Y. Wang, *J. Power Sources* **2016**, 329, 339.
- [154] T. Aida, K. Yamada, M. Morita, *Electrochim. Solid-State Lett.* **2006**, 9, A534.
- [155] W. Cao, J. Zheng, D. Adams, T. Doung, J. P. Zheng, *J. Electrochem. Soc.* **2014**, 161, A2087.
- [156] T. Aida, I. Murayama, K. Yamada, M. Morita, *J. Electrochim. Soc.* **2007**, 154, A798.
- [157] T. Aida, I. Murayama, K. Yamada, M. Morita, *Electrochim. Solid-State Lett.* **2007**, 10, A93.
- [158] T. Aida, I. Murayama, K. Yamada, M. Morita, *J. Power Sources* **2007**, 166, 462.
- [159] W. J. Cao, J. P. Zheng, *ECS Trans.* **2013**, 45, 165.
- [160] W. J. Cao, J. P. Zheng, *J. Electrochim. Soc.* **2013**, 160, A1572.
- [161] W. J. Cao, Y. X. Li, B. Fitch, J. Shih, T. Doung, J. P. Zheng, *ECS Trans.* **2015**, 64, 67.
- [162] W. J. Cao, M. Greenleaf, Y. X. Li, D. Adams, M. Hagen, T. Doung, J. P. Zheng, *J. Power Sources* **2015**, 280, 600.
- [163] W. J. Cao, J. F. Luo, J. Yan, X. J. Chen, W. Brandt, M. Warfield, D. Lewis, S. R. Yturriaga, D. G. Moye, J. P. Zheng, *J. Electrochim. Soc.* **2017**, 164, A93.
- [164] X. Sun, X. Zhang, W. Liu, K. Wang, C. Li, Z. Li, Y. Ma, *Electrochim. Acta* **2017**, 235, 158.
- [165] J. Zhang, X. Liu, J. Wang, J. Shi, Z. Shi, *Electrochim. Acta* **2016**, 187, 134.
- [166] Y.-N. Jo, M.-S. Park, E.-Y. Lee, J.-G. Kim, K.-J. Hong, S.-I. Lee, H. Y. Jeong, G. H. Ryu, Z. Lee, Y.-J. Kim, *Electrochim. Acta* **2014**, 146, 630.
- [167] M. Schroeder, S. Menne, J. Ségalini, D. Saurel, M. Casas-Cabanas, S. Passerini, M. Winter, A. Balducci, *J. Power Sources* **2014**, 266, 250.
- [168] M. Schroeder, M. Winter, S. Passerini, A. Balducci, *J. Electrochim. Soc.* **2012**, 159, A1240.
- [169] M. Schroeder, M. Winter, S. Passerini, A. Balducci, *J. Power Sources* **2013**, 238, 388.
- [170] A. Yoshino, T. Tsubata, M. Shimoyamada, H. Satake, Y. Okano, S. Mori, S. Yata, *J. Electrochim. Soc.* **2004**, 151, A2180.
- [171] Y.-G. Lim, M.-S. Park, K. J. Kim, K.-S. Jung, J. H. Kim, M. Shahabuddin, D. Byun, J.-S. Yu, *J. Power Sources* **2015**, 299, 49.
- [172] J.-Y. Li, Q. Xu, G. Li, Y.-X. Yin, L.-J. Wan, Y.-G. Guo, *Mater. Chem. Front.* **2017**, 1, 1691.
- [173] B. Li, F. Dai, Q. Xiao, L. Yang, J. Shen, C. Zhang, M. Cai, *Adv. Energy Mater.* **2016**, 6, 1600802.
- [174] C.-M. Lai, T.-L. Kao, H.-Y. Tuan, *J. Power Sources* **2018**, 379, 261.
- [175] D. A. C. Brownson, D. K. Kampouris, C. E. Banks, *J. Power Sources* **2011**, 196, 4873.
- [176] H.-J. Choi, S.-M. Jung, J.-M. Seo, D. W. Chang, L. Dai, J.-B. Baek, *Nano Energy* **2012**, 1, 534.
- [177] R. K. L. Tan, S. P. Reeves, N. Hashemi, D. G. Thomas, E. Kavak, R. Montazami, N. N. Hashemi, *J. Mater. Chem. A* **2017**, 5, 17777.
- [178] R. Thangavel, B. Moorthy, D. K. Kim, Y.-S. Lee, *Adv. Energy Mater.* **2017**, 7, 1602654.
- [179] J. H. Lee, W. H. Shin, M.-H. Ryoo, J. K. Jin, J. Kim, J. W. Choi, *ChemSusChem* **2012**, 5, 2328.
- [180] M. M. Hantel, T. Kaspar, R. Nesper, A. Wokaun, R. Kötz, *ECS Electrochim. Lett.* **2012**, 1, A1.
- [181] J. Zhang, W. Lv, D. Zheng, Q. Liang, D.-W. Wang, F. Kang, Q.-H. Yang, *Adv. Energy Mater.* **2018**, 8, 1702395.
- [182] Y. W. Zhu, S. Murali, M. D. Stoller, K. J. Ganesh, W. W. Cai, P. J. Ferreira, A. Pirkle, R. M. Wallace, K. A. Cybosz, M. Thommes, D. Su, E. A. Stach, R. S. Ruoff, *Science* **2011**, 332, 1537.
- [183] F. Tu, S. Liu, T. Wu, G. Jin, C. Pan, *Powder Technol.* **2014**, 253, 580.

- [184] T. Zhang, F. Zhang, L. Zhang, Y. Lu, Y. Zhang, X. Yang, Y. Ma, Y. Huang, *Carbon* **2015**, 92, 106.
- [185] X. Yu, C. Zhan, R. Lv, Y. Bai, Y. Lin, Z.-H. Huang, W. Shen, X. Qiu, F. Kang, *Nano Energy* **2015**, 15, 43.
- [186] W. Ahn, D. U. Lee, G. Li, K. Feng, X. Wang, A. Yu, G. Lui, Z. Chen, *ACS Appl. Mater. Interfaces* **2016**, 8, 25297.
- [187] X.-Y. Shan, Y. Wang, D.-W. Wang, F. Li, H.-M. Cheng, *Adv. Energy Mater.* **2016**, 6, 1502064.
- [188] Y.-Z. Wang, X.-Y. Shan, D.-W. Wang, C.-M. Chen, F. Li, H.-M. Cheng, *Asia-Pac. J. Chem. Eng.* **2016**, 11, 407.
- [189] J. R. Rani, R. Thangavel, S.-I. Oh, J. M. Woo, N. C. Das, S.-Y. Kim, Y.-S. Lee, J.-H. Jang, *ACS Appl. Mater. Interfaces* **2017**, 9, 22398.
- [190] Y. Tao, X. Xie, W. Lv, D.-M. Tang, D. Kong, Z. Huang, H. Nishihara, T. Ishii, B. Li, D. Golberg, F. Kang, T. Kyotani, Q.-H. Yang, *Sci. Rep.* **2013**, 3, 2975.
- [191] V. H. Pham, J. H. Dickerson, *J. Phys. Chem. C* **2016**, 120, 5353.
- [192] Y. Xu, Z. Lin, X. Zhong, X. Huang, N. O. Weiss, Y. Huang, X. Duan, *Nat. Commun.* **2014**, 5, 4554.
- [193] L. Jiang, L. Sheng, C. Long, T. Wei, Z. Fan, *Adv. Energy Mater.* **2015**, 5, 1500771.
- [194] Z. Liu, Y. G. Andreev, A. R. Armstrong, S. Brutti, Y. Ren, P. G. Brucea, *Prog. Nat. Sci.: Mater. Int.* **2013**, 23, 235.
- [195] H. Kim, M.-Y. Cho, M.-H. Kim, K.-Y. Park, H. Gwon, Y. Lee, K. C. Roh, K. Kang, *Adv. Energy Mater.* **2013**, 3, 1500.
- [196] V. Aravindan, N. Shubha, W. C. Ling, S. Madhavi, *J. Mater. Chem. A* **2013**, 1, 6145.
- [197] H. Wang, C. Guan, X. Wang, H. J. Fan, *Small* **2015**, 11, 1470.
- [198] D. Wang, K. Xie, Y. Wang, S. Cheng, *Int. J. Electrochem. Sci.* **2016**, 11, 9776.
- [199] J. H. Kim, H. J. Choi, H.-K. Kim, S.-H. Lee, Y.-H. Lee, *Int. J. Hydrogen Energy* **2016**, 41, 13549.
- [200] F. Wang, C. Wang, Y. Zhao, Z. Liu, Z. Chang, L. Fu, Y. Zhu, Y. Wu, D. Zhao, *Small* **2016**, 12, 6207.
- [201] V. Aravindan, M. V. Reddy, S. Madhavi, S. G. Mhaisalkar, G. V. Subba Rao, B. V. R. Chowdari, *J. Power Sources* **2011**, 196, 8850.
- [202] H. Li, L. Shen, J. Wang, S. Fang, Y. Zhang, H. Dou, X. Zhang, *J. Mater. Chem. A* **2015**, 3, 16785.
- [203] X. Wang, G. Shen, *Nano Energy* **2015**, 15, 104.
- [204] J.-M. Li, K.-H. Chang, T.-H. Wu, C.-C. Hu, *J. Power Sources* **2013**, 224, 59.
- [205] Z. Chen, V. Augustyn, J. Wen, Y. Zhang, M. Shen, B. Dunn, Y. Lu, *Adv. Mater.* **2011**, 23, 791.
- [206] G. Li, X. Wang, F. M. Hassan, M. Li, R. Batmaz, X. Xiao, A. Yu, *ChemElectroChem* **2015**, 2, 1264.
- [207] L. Cheng, H.-Q. Li, Y.-Y. Xia, *J. Solid State Electrochem.* **2006**, 10, 405.
- [208] X. Zhao, C. Johnston, P. S. Grant, *J. Mater. Chem.* **2009**, 19, 8755.
- [209] A. Brandt, A. Balducci, *Electrochim. Acta* **2013**, 108, 219.
- [210] X. Yu, J. Deng, C. Zhan, R. Lv, Z.-H. Huang, F. Kang, *Electrochim. Acta* **2017**, 228, 76.
- [211] F. Zhang, T. Zhang, X. Yang, L. Zhang, K. Leng, Y. Huang, Y. Chen, *Energy Environ. Sci.* **2013**, 6, 1623.
- [212] M. Yang, Y. Zhong, J. Ren, X. Zhou, J. Wei, Z. Zhou, *Adv. Energy Mater.* **2015**, 5, 1500550.
- [213] C. Liu, C. Zhang, H. Song, X. Nan, H. Fu, G. Cao, *J. Mater. Chem. A* **2016**, 4, 3362.
- [214] C. Liu, C. Zhang, H. Song, C. Zhang, Y. Liu, X. Nan, G. Cao, *Nano Energy* **2016**, 22, 290.
- [215] M. Ulaganathan, V. Aravindan, W. C. Ling, Q. Yan, S. Madhavi, *J. Mater. Chem. A* **2016**, 4, 15134.
- [216] J. Zhang, H. Chen, X. Sun, X. Kang, Y. Zhang, C. Xu, Y. Zhang, *J. Electrochem. Soc.* **2017**, 164, A820.
- [217] L. P. Wang, L. Yu, R. Satish, J. Zhu, Q. Yan, M. Srinivasan, Z. Xu, *RSC Adv.* **2014**, 4, 37389.
- [218] E. Lim, C. Jo, H. Kim, M.-H. Kim, Y. Mun, J. Chun, Y. Ye, J. Hwang, K.-S. Ha, K. C. Roh, K. Kang, S. Yoon, J. Lee, *ACS Nano* **2015**, 9, 7497.
- [219] S. Liu, J. Zhou, Z. Cai, G. Fang, Y. Cai, A. Pan, S. Liang, *J. Mater. Chem. A* **2016**, 4, 17838.
- [220] H. Song, J. Fu, K. Ding, C. Huang, K. Wu, X. Zhang, B. Gao, K. Huo, X. Peng, P. K. Chu, *J. Power Sources* **2016**, 328, 599.
- [221] G. Ma, K. Li, Y. Li, B. Gao, T. Ding, Q. Zhong, J. Su, L. Gong, J. Chen, L. Yuan, B. Hu, J. Zhou, K. Huo, *ChemElectroChem* **2016**, 3, 1360.
- [222] J. Wang, H. Li, L. Shen, S. Dong, X. Zhang, *RSC Adv.* **2016**, 6, 71338.
- [223] H. Yang, H. Xu, L. Wang, L. Zhang, Y. Huang, X. Hu, *Chem. – Eur. J.* **2017**, 23, 4203.
- [224] W. Li, B. Song, A. Manthiram, *Chem. Soc. Rev.* **2017**, 46, 3006.
- [225] D. Cericola, P. Novák, A. Wokaun, R. Kötz, *Electrochim. Acta* **2011**, 56, 8403.
- [226] D. Cericola, P. W. Ruch, R. Kötz, P. Novák, A. Wokaun, *Electrochim. Commun.* **2010**, 12, 812.
- [227] N. Böckenfeld, R.-S. Kühnle, S. Passerini, M. Winter, A. Balducci, *J. Power Sources* **2011**, 196, 4136.
- [228] L. N. Ping, J. M. Zheng, Z. Q. Shi, J. Qi, C. Y. Wang, *Chin. Sci. Bull.* **2013**, 58, 689.
- [229] X. Sun, X. Zhang, B. Huang, H. Zhang, D. Zhang, Y. Ma, *J. Power Sources* **2013**, 243, 361.
- [230] X. Sun, X. Zhang, H. Zhang, N. Xu, K. Wang, Y. Ma, *J. Power Sources* **2014**, 270, 318.
- [231] M. Hagen, W. J. Cao, A. Shellikeri, D. Adams, X. J. Chen, W. Brandt, S. R. Yturriaga, Q. Wu, J. A. Read, T. R. Jow, J. P. Zheng, *J. Power Sources* **2018**, 379, 212.
- [232] X. B. Hu, Y. J. Huai, Z. J. Lin, J. S. Suo, Z. H. Deng, *J. Electrochim. Soc.* **2007**, 154, A1026.
- [233] X. Hu, Z. Deng, J. Suo, Z. Pan, *J. Power Sources* **2009**, 187, 635.
- [234] D. Cericola, P. Novák, A. Wokaun, R. Kötz, *J. Power Sources* **2011**, 196, 10305.
- [235] Y. Lei, Z.-H. Huang, W. Shen, F. Kang, Y. Zheng, *Electrochim. Acta* **2013**, 107, 413.
- [236] H. Wu, C. V. Rao, B. Rambabu, *Mater. Chem. Phys.* **2009**, 116, 532.
- [237] A. Brandt, A. Balducci, U. Rodehorst, S. Menne, M. Winter, A. Bhaskar, *J. Electrochim. Soc.* **2014**, 161, A1139.
- [238] N. Arun, A. Jain, V. Aravindan, S. Jayaraman, W. C. Ling, M. P. Srinivasan, S. Madhavi, *Nano Energy* **2015**, 12, 69.
- [239] J. Li, X. Zhang, R. Peng, Y. Huang, L. Guo, Y. Qi, *RSC Adv.* **2016**, 6, 54866.
- [240] J.-H. Yoon, H. J. Bang, J. Prakash, Y.-K. Sun, *Mater. Chem. Phys.* **2008**, 110, 222.
- [241] A. Krause, P. Kosyrev, M. Oljaca, S. Passerini, M. Winter, A. Balducci, *J. Power Sources* **2011**, 196, 8836.
- [242] K. Karthikeyan, V. Aravindan, S. B. Lee, I. C. Jang, H. H. Lim, G. J. Park, M. Yoshio, Y. S. Lee, *J. Power Sources* **2010**, 195, 3761.
- [243] K. Karthikeyan, S. Amaresh, V. Aravindan, H. Kim, K. S. Kang, Y. S. Lee, *J. Mater. Chem. A* **2013**, 1, 707.
- [244] K. Karthikeyan, S. Amaresh, K. J. Kim, S. H. Kim, K. Y. Chung, B. W. Cho, Y. S. Lee, *Nanoscale* **2013**, 5, 5958.
- [245] M. Sevilla, R. Mokay, *Energy Environ. Sci.* **2014**, 7, 1250.
- [246] A. D. Pasquier, A. Laforgue, P. Simon, G. G. Amatucci, J.-F. Fauvarque, *J. Power Sources* **2002**, 149, A302.
- [247] A. D. Pasquier, A. Laforgue, P. Simonc, *J. Power Sources* **2004**, 125, 95.
- [248] K. Kaliyappan, S. Amaresh, Y.-S. Lee, *ACS Appl. Mater. Interfaces* **2014**, 6, 11357.
- [249] K. Karthikeyan, S. Amaresh, S.-N. Lee, J.-Y. An, Y.-S. Lee, *ChemSusChem* **2014**, 7, 2310.
- [250] P. Chang, C. Wang, T. Kinumoto, T. Tsumura, M. Chen, M. Toyoda, *ChemElectroChem* **2017**, 4, 1.

- [251] P.-P. Chang, K. Matsumura, C.-Y. Wang, T. Kinumoto, T. Tsumura, M.-M. Chen, M. Toyoda, *Carbon* **2016**, *108*, 225.
- [252] Z.-J. Qiao, M.-M. Chen, C.-Y. Wang, Y.-C. Yuan, *Bioresour. Technol.* **2014**, *163*, 386.
- [253] K.-W. Nam, S.-B. Ma, W.-S. Yoon, X.-Q. Yang, K.-B. Kim, *Electrochem. Commun.* **2009**, *11*, 1166.
- [254] Y. Yue, P. Han, X. He, K. Zhang, Z. Liu, C. Zhang, S. Dong, L. Gu, G. Cui, *J. Mater. Chem.* **2012**, *22*, 4938.
- [255] K. Zhang, P. Han, L. Gu, L. Zhang, Z. Liu, Q. Kong, C. Zhang, S. Dong, Z. Zhang, J. Yao, H. Xu, G. Cui, L. Chen, *ACS Appl. Mater. Interfaces* **2012**, *4*, 658.
- [256] A. Laheäär, H. Kurig, A. Jänes, E. Lust, *Electrochim. Acta* **2009**, *54*, 4587.
- [257] M. A. Azam, N. H. Jantan, N. Dorah, R. N. A. R. Seman, N. S. A. Manaf, T. I. T. Kudin, M. Z. A. Yahya, *Mater. Res. Bull.* **2015**, *69*, 20.
- [258] R. V. Salvatierra, D. Zakhidov, J. Sha, N. D. Kim, S.-K. Lee, A.-R. O. Raji, N. Zhao, J. M. Tour, *ACS Nano* **2017**, *11*, 2724.
- [259] R. Chen, W. Qu, X. Guo, L. Li, F. Wu, *Mater. Horiz.* **2016**, *3*, 487.
- [260] X. Lu, M. Yu, G. Wang, Y. Tong, Y. Li, *Energy Environ. Sci.* **2014**, *7*, 2160.
- [261] Y.-D. Chiou, D.-S. Tsai, H. H. Lam, C.-H. Chang, K.-Y. Lee, Y.-S. Huang, *Nanoscale* **2013**, *5*, 8122.
- [262] W. Na, A. S. Lee, J. H. Lee, S. S. Hwang, S. M. Hong, E. Kim, C. M. Koo, *Electrochim. Acta* **2016**, *188*, 582.
- [263] H. Wang, Y. Zhang, H. Ang, Y. Zhang, H. T. Tan, Y. Zhang, Y. Guo, J. B. Franklin, X. L. Wu, M. Srinivasan, H. J. Fan, Q. Yan, *Adv. Funct. Mater.* **2016**, *26*, 3082.
- [264] B. Anasori, M. R. Lukatskaya, Y. Gogotsi, *Nat. Rev. Mater.* **2017**, *2*, 16098.
- [265] N. K. Chaudhari, H. Jin, B. Kim, D. S. Baek, S. H. Joo, K. Lee, *J. Mater. Chem. A* **2017**, *5*, 24564.
- [266] V. M. Hong Ng, H. Huang, K. Zhou, P. S. Lee, W. Que, J. Z. Xu, L. B. Kong, *J. Mater. Chem. A* **2017**, *5*, 3039.
- [267] A. Byeon, A. M. Glushenkov, B. Anasori, P. Urbankowski, J. Li, B. W. Byles, B. Blake, K. L. Van Aken, S. Kota, E. Pomerantseva, J. W. Lee, Y. Chen, Y. Gogotsi, *J. Power Sources* **2016**, *326*, 686.
- [268] J. Luo, W. Zhang, H. Yuan, C. Jin, L. Zhang, H. Huang, C. Liang, Y. Xia, J. Zhang, Y. Gan, X. Tao, *ACS Nano* **2017**, *11*, 2459.
- [269] P. Yu, G. Cao, S. Yi, X. Zhang, C. Li, X. Sun, K. Wang, Y. Ma, *Nanoscale* **2018**, *10*, 5906.
- [270] G. Zhang, H. Liu, J. Qu, J. Li, *Energy Environ. Sci.* **2016**, *9*, 1190.
- [271] H.-Y. Wei, D.-S. Tsai, C.-L. Hsieh, *RSC Adv.* **2015**, *5*, 69176.
- [272] L. Shen, H. Lv, S. Chen, P. Kopold, P. A. Van Aken, X. Wu, J. Maier, Y. Yu, *Adv. Mater.* **2017**, *29*, 1700142.
- [273] F. Wang, Z. Liu, X. Yuan, J. Mo, C. Li, L. Fu, Y. Zhu, X. Wu, Y. Wu, *J. Mater. Chem. A* **2017**, *5*, 14922.
- [274] J. Yan, W. J. Cao, J. P. Zheng, *J. Electrochem. Soc.* **2017**, *164*, A2164.
- [275] K. Yao, W. J. Cao, R. Liang, J. P. Zheng, *J. Electrochem. Soc.* **2017**, *164*, A1480.
- [276] R. Wang, J. Lang, P. Zhang, Z. Lin, X. Yan, *Adv. Funct. Mater.* **2015**, *25*, 2270.
- [277] J.-M. Jiang, P. Nie, S.-Y. Dong, Y.-T. Wu, X.-G. Zhang, *Acta Phys.-Chim. Sin.* **2017**, *33*, 780.
- [278] G. Gourdin, P. H. Smith, T. Jiang, T. N. Tran, D. Qu, *J. Electroanal. Chem.* **2013**, *688*, 103.
- [279] T. Shinichi, A. Nobuo, N. Mitsuru, S. Mitsuo, M. Kohei, H. Yukinori (Fuji Heavy Ind Ltd), *Japan* 2005-104676, **2005**.
- [280] K. Koji (TAIYO YUDEN Co Ltd), *Japan* 2012-169061, **2012**.
- [281] W. J. Cao, J. Shih, J. P. Zheng, T. Doung, *J. Power Sources* **2014**, *257*, 388.
- [282] M. Yuan, W. Liu, Y. Zhu, Y. Xu, *Russ. J. Electrochem.* **2014**, *50*, 1050.
- [283] S. Kumagai, T. Ishikawa, N. Sawa, *J. Energy Storage* **2015**, *2*, 1.
- [284] M.-S. Park, Y.-G. Lim, J.-W. Park, J.-S. Kim, J.-W. Lee, J. H. Kim, S. X. Dou, Y.-J. Kim, *J. Phys. Chem. C* **2013**, *117*, 11471.
- [285] M.-S. Park, Y.-G. Lim, S. M. Hwang, J. H. Kim, J.-S. Kim, S. X. Dou, J. Cho, Y.-J. Kim, *ChemSusChem* **2014**, *7*, 3138.
- [286] Y.-G. Lim, D. Kim, J.-M. Lim, J.-S. Kim, J.-S. Yu, Y.-J. Kim, D. Byun, M. Cho, K. Cho, M.-S. Park, *J. Mater. Chem. A* **2015**, *3*, 12377.
- [287] P. Jeżowski, K. Fic, O. Crosnier, T. Brousse, F. Béguin, *Electrochim. Acta* **2016**, *206*, 440.
- [288] P. Jeżowski, K. Fic, O. Crosnier, T. Brousse, F. Béguin, *J. Mater. Chem. A* **2016**, *4*, 12609.